We thank the editor and reviewers for their valuable comments. We have replied the comments one by one below, and revised the manuscript accordingly. The replies are highlighted in blue color and the modified texts (in the revised manuscript) are shown italic.

The Editor's comment

I have received two reviews of your manuscript. As you can see, both of them are very positive. But I would like to recommend for addressing the uncertainty in streamflow simulation, e.g., excluding those with NSE<0 simulations to see whether it affects main conclusions?

Reply: Thanks for the suggestion. Please note that the station data are only used for evaluating the multimodel simulations. We have re-calculated the average streamflow of stations over individual basins and China by excluding those with NSE<0 and redrawn the related figures (see Figures R1, R2 and R3). The inner plot in Figure R1, showing the observed and simulated streamflow seasonality of stations with NSE>0 (see Table S2) over China, has very little change compared to Figure 1 in the revised manuscript. In several northern basins (especially the Liao River), the seasonal streamflow (Figure R2) and annual streamflow (Figure R3) of the stations shows some differences from Figure S2 and S3 (in the revised manuscript). That is, the simulations and observations of the selected stations (NSE>0) are closer in these basins. Generally, the excluding of those stations do not have large effects because the excluded streamflows are relatively small. As the stations with NSE<0 are located in the northern basins (see Figure S2 below), the redrawn plots for the southern basins have no change.

In this study, we would like to use all station data for the evaluation. Excluding those stations with NSE<0 only affects the evaluation result, and would not affect the conclusions about the human and climate impacts on streamflow in China.

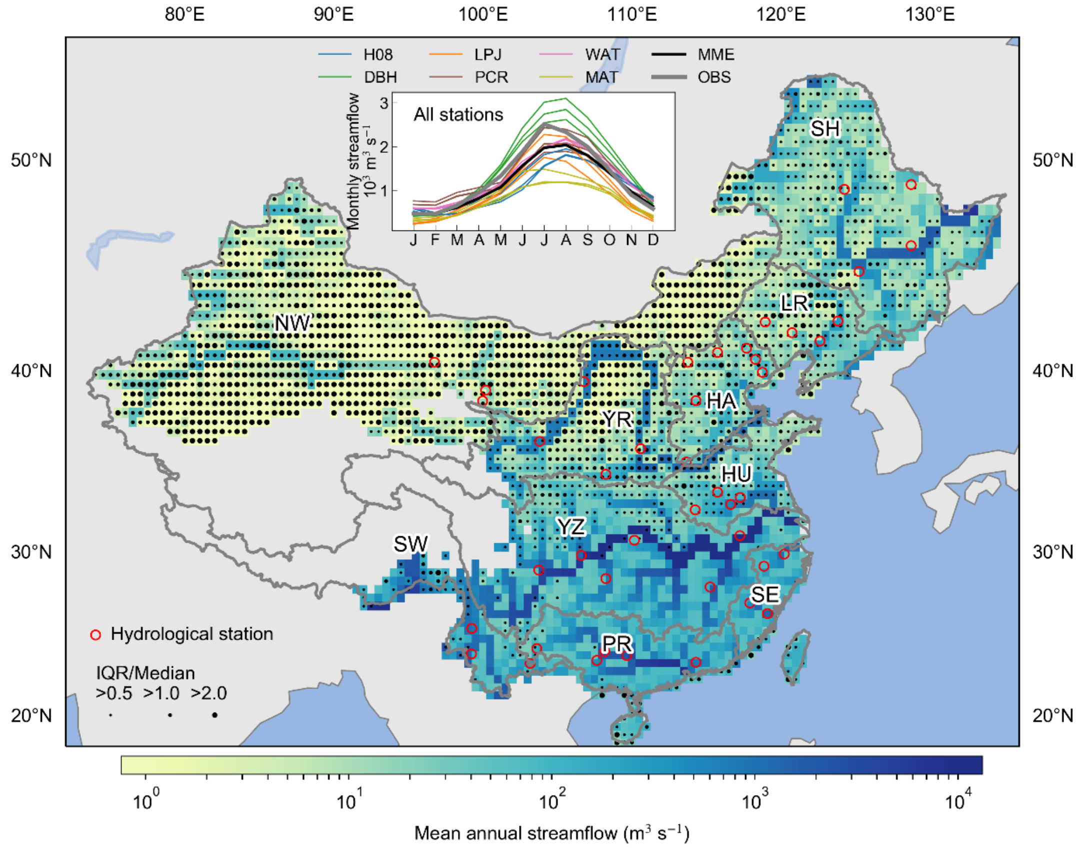

Figure R1. Multimodel medians of mean annual streamflow (MAF) in China from the VARSOC experiment. MAF medians are computed across 18 GHM-GMF combinations over the 1971-2000 period. The ensemble spread is represented by the ratio of interquartile range (IQR, 75th percentile minus 25th percentile) to the ensemble median of MAF (Median). The red circles indicate hydrological stations. The inner plot shows the comparison of the simulated seasonal streamflow (each GHM has three lines for the three GMFs) from the VARSOC experiment against the observations averaged for the hydrological stations with NSE>0 (see Table S2) over the period 1971-2000. The GHM names and basin names are the same as Figure 1 in the revised manuscript.

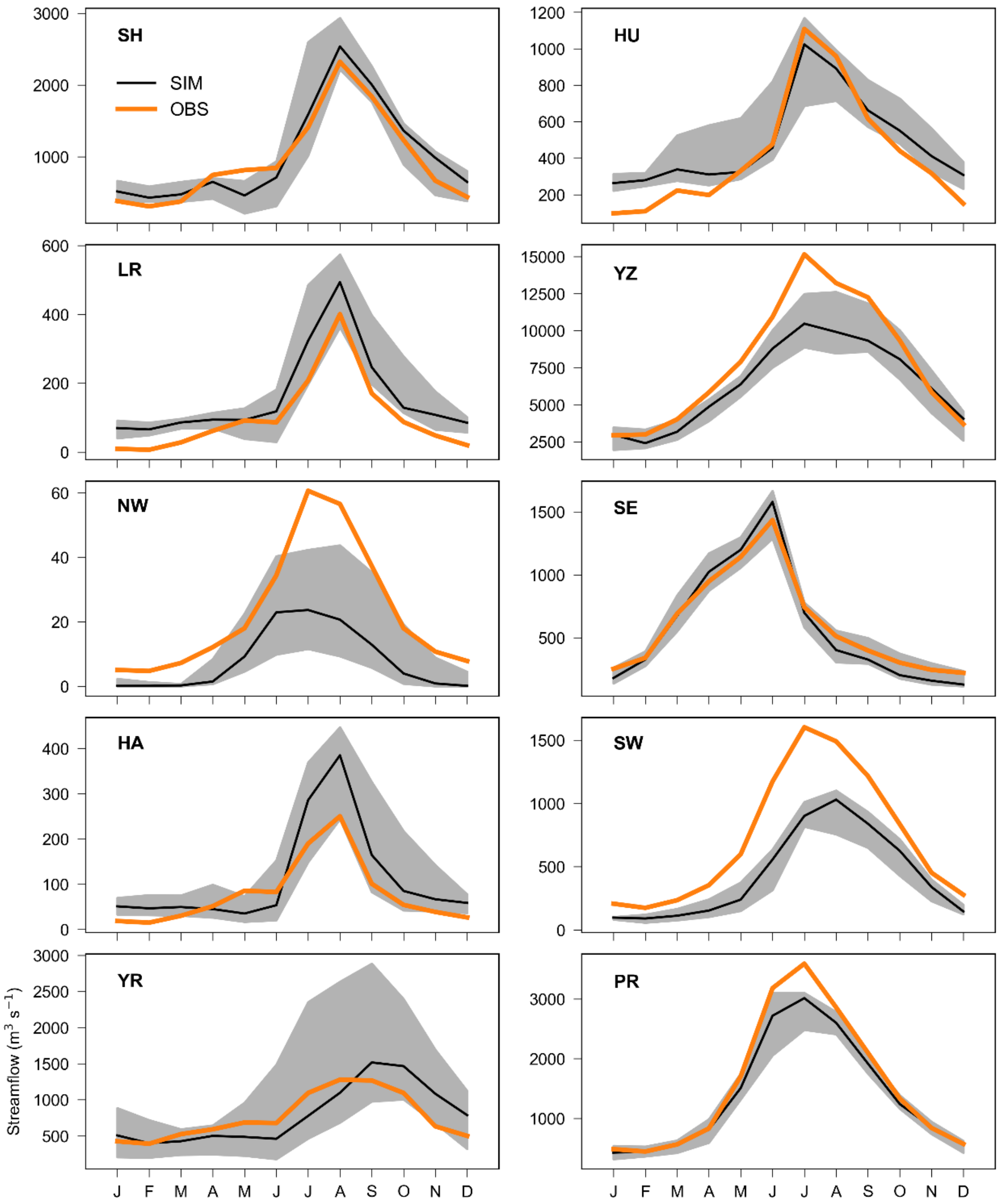

Figure R2. Seasonal cycle of streamflow from observations (orange) and multimodel medians (black). The observations are the average values of the hydrological stations with NSE > 0 (see Table S2), while the simulations are averaged values over the grid cells identified by the location of stations. The grey areas show the 25th and 75th percentiles of the multimodel simulations. Northern basins: Songhua River (SH), Liao River (LR), Northwest Rivers (NW), Hai River (HA), Yellow River (YR), Huai River (HU); Southern basins: Yangtze River (YZ), Southeast Rivers (SE), Southwest Rivers (SW), Pearl River (PR).

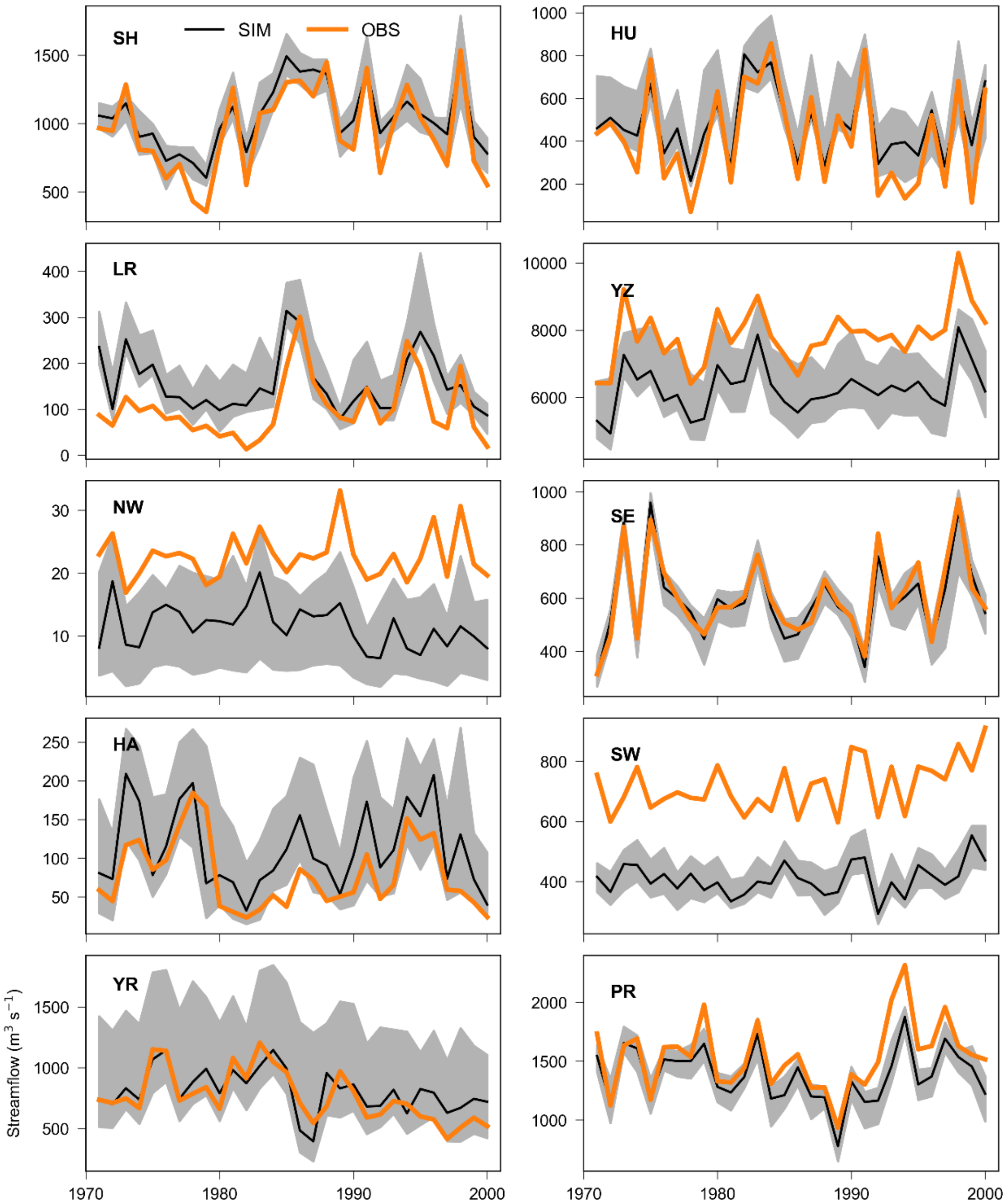

Figure R3. Simulated (black) and observed (orange) mean annual streamflow at the hydrological stations in each basin. The observations are the average values of the hydrological stations with NSE>0 (see Table S2), while the simulations are averaged values over the grid cells identified by the location of stations. The gray areas show the 25th and 75th percentiles of the multimodel simulations.

Reviewer #1

This study quantitative assessed the human impact and climate change impact on streamflow in continental China. The simulations streamflow was used from six global hydrological models driven by three meteorological forcings. The research is very interesting and significative. However, there are a few issues that the authors need to address before the manuscript can be accepted. I recommend most of the issues I raise below just need clarification or justification.
Reply: Thanks for the positive comment. We have replied the comments below and revised manuscript accordingly.

1. The simulated results need to be verified further with observed streamflow, maybe, QQPLOT, NSE etc. method can be used.
Reply: We have calculated NSE for the 44 stations, and added a sentence describing the result with a table (new added Table S2) in the revised supplementary information.

Revision in the manuscript (Subsection 3.1, the second paragraph (new added)):
The Nash-Sutcliffe coefficients calculated for the multimodel median and observed monthly streamflow at each station (see Table S2) show that the multimodel medians have better performance in the southern basins.

Table S2. The Nash-Sutcliffe coefficients (NSE) for the simulated monthly streamflow from VARSOC experiment and observed monthly streamflow ($m^3 s^{-1}$) at the 44 stations over the 1971-2000 period. The observed mean annual streamflow (MAF, $m^3 s^{-1}$) averaged over the period is also shown for each station.

Number	Station Name	MAF	NSE	River name	Number	Station Name	MAF	NSE	River name
1	Guchengzi	151.26	-0.27	Songhua River	23	Xixian	117.87	0.31	Huai River
2	Fuyu	449.68	0.53	Songhua River	24	Fuyang	117.74	0.63	Huai River
3	Tonghe	1444.43	0.81	Songhua River	25	Lutaizi	639.00	0.80	Huai River
4	Kuerbin	26.94	0.004	Songhua River	26	Bengbu	800.63	0.81	Huai River
5	Chaoyang	18.00	-0.88	Liao River	27	Shishang	1968.28	0.93	Yangtze River
6	Chifeng	7.76	-0.25	Liao River	28	Changyang	431.02	0.75	Yangtze River
7	Tieling	84.36	<-1.0	Liao River	29	Pingshan	4546.38	0.77	Yangtze River
8	Liaozhong	101.43	0.50	Liao River	30	Sinan	910.98	0.79	Yangtze River
9	Changmapu	29.30	-0.37	Northwest Rivers	31	Cuntan	10747.92	0.68	Yangtze River
10	Yingluoxia	51.06	-0.26	Northwest Rivers	32	Datong	28460.19	0.78	Yangtze River
11	Zhamashenke	22.70	0.09	Northwest Rivers	33	Quzhou	207.66	0.80	Southeast Rivers
12	Sandaohezi	16.45	<-1.0	Hai River	34	Zhuji	40.24	0.58	Southeast Rivers
13	Panjiakou	60.87	0.01	Hai River	35	Zhuqi	1721.14	0.91	Southeast Rivers
14	Luanxian	96.09	0.71	Hai River	36	Yangkou	442.85	0.72	Southeast Rivers
15	Xiapu	4.58	<-1.0	Hai River	37	Daojieba	1746.97	0.12	Southwest Rivers
16	Huangbizhuang	32.14	-0.07	Hai River	38	Gulaohe	96.63	0.22	Southwest Rivers
17	Cetian	4.78	-0.01	Hai River	39	Manhao	310.84	0.82	Southwest Rivers
18	Lanzhou	976.80	0.53	Yellow River	40	Jiangbianjie	194.96	0.68	Pearl River
19	Shizuishan	867.25	0.45	Yellow River	41	Duanzhan	2005.11	0.88	Pearl River
20	Longmen	803.67	-0.47	Yellow River	42	Xiayan	449.63	0.82	Pearl River
21	Huayuankou	1103.51	0.09	Yellow River	43	Wuxuan	4130.25	0.81	Pearl River
22	Xianyang	107.26	0.63	Yellow River	44	Boluo	782.04	0.80	Pearl River

2. The simulated results are very bad in some basins, such as NW, SW, HA. These simulated streamflow need be post-processed, and then be used to analyzed the impact of human and climate change.

Reply: We recognized the poor performance of the simulations, especially in the northern basins (see above Table S2). A post-processing on the simulations could reduce the deviation in simulated streamflow from observations and narrow the spread across models (e.g., Yin et al., 2017). However, in this study, there are only limited stations (e.g., three stations in the Northwest Rivers and two stations in the Southwest Rivers) which cover small areas. If the limited number of the stations were used to correct the whole Northwest or Southwest regions, we found it would lead to very unrealistic streamflow estimates over rivers that we do not have streamflow observations (but know the mean annual streamflow from the reported statistics). Furthermore, the estimated water withdrawals in the models may be affected by the streamflow estimates. We would like to keep it consistent with water withdrawal estimates by the models. Due to the above reasons, we decided not to post-process the streamflow estimates. We have added a caution for the limited representative of the observations in the evaluation result to remind readers to treat it carefully.

Revision in the manuscript (Subsection 3.1, the second paragraph (new added)):

It should be noted that the stations are located at different reaches of individual basins. *Thus, the station-averaged estimates are largely dominated by those with large streamflow (e.g., at the lower reaches). Additionally, the coverage of stations used is relatively small (due to data availability), especially in hydrologically variable regions like in the Northwest Rivers, leading to not necessarily representative evaluation of the performance of the GHMs in the whole basin.*

3. The authors need add some explanation of ISIMIP2a about how to simulate water withdrawals.

Reply: We have added some description for the simulated water withdrawals in section 2.1 Simulation data.

Revision in the manuscript (Subsection 2.1, the second paragraph (new added)):

Human impact considered in the VARSOC experiment (see the maps in Figure S1 and Table S1 for more details) includes the time-varying areas for both irrigated and rainfed cropland (Fader et al., 2010; Portmann et al., 2010) and reservoirs (dams) from the Global Reservoir and Dam (GRanD) Database (Lehner et al., 2011) including their commissioning year (see Figure S1 and Table S1 for more detail). Reservoir regulation was considered in the VARSOC experiment, which often reduces high streamflow in high-flow seasons and increases streamflow in dry seasons (Masaki, et al., 2017). Inter-basin water transfer was not considered in any of the model runs. The simulations of water withdrawals are different between the GHMs with respect to water use requirements and water withdrawal sources which are shown in Table S1. The sources of water withdrawals, depending on models, may include river channel, reservoirs, groundwater and lakes, and their fractions can be determined from reported statistics (e.g., Siebert et al., 2010) or estimated in models (Wada et al., 2014). In addition to the irrigation water requirement which is usually estimated by coupling crop models, most

GHMs considered the requirements for domestic and industrial water use which were prescribed in H08 (Hanasaki et al., 2008), LPJmL and MATSIRO (Pokhrel et al., 2015) or were estimated according to the population, socioeconomic and technological development in PCR-GLOBWB (Wada et al., 2014) and the population, thermal electricity production, gross added value, and technological change in WaterGAP (Flörke et al., 2013). Water use requirement for livestock was also prescribed in the LPJmL model, and estimated according to livestock densities in PCR-GLOBWB and WaterGAP2.

Reviewer #2

The paper describes a multimodel assessment of the relative impacts of human activities and climate on mean annual streamflow over the past 4 decades in China. This study shows that unlike previous assessments, the climate impact signal is much more pronounced than the human impact signal in 88% of river segments in China. The study also quantifies the impact of humans across basins and discusses regional differences. In general the paper is publishable after some moderate revisions.

Reply: Thanks for the positive comments. We have replied the comments and revised the manuscript accordingly.

- The use of the term 'climate change' in the title and throughout the manuscript is somewhat confusing and misleading because it gives the impression that the paper will be forward looking in time and over the coming several decades (e.g., 2050, 2100). A more appropriate term is 'climate impacts'

Reply: We used "climate impact" in the title. We have replaced "climate change" by "climate variability" in most cases, and by "climate impact" in some cases where appropriate. "climate change" is still used when it refers to future climate change and results from some specific references.

- The 3rd paragraph of the introduction makes the argument that "This is the first study to perform such a quantitative assessment for all rivers of China with comparable modeling experiments." Being aware of the ISIMIP publications (https://www.isimip.org/outcomes/publications/) in this space with global assessments including many of the authors on this paper, I find this argument to be an exaggeration. I think the last sentence of that paragraph is a key novelty of this work, and as such linking back to the content of the second paragraph in the introduction to make the case would be my suggestion. I do agree that focusing on China is somewhat unique about this study. So one suggestion is to tweak the noted sentence as follow "This is the first study to focus on performing such a quantitative assessment for all rivers of China with comparable modeling experiments."

o Schewe et al.: Multimodel assessment of water scarcity under climate change. PNAS, 2014.

o Haddeland et al.: Global water resources affected by human interventions and climate change, P. Natl. Acad. Sci. USA, 111, 3251–3256, https://doi.org/10.1073/pnas.1222475110, 2014.

o Veldkamp et al.: Water scarcity hotspots travel downstream due to human interventions in the 20th and 21st century, Nature Commun., 8, 15697, https://doi.org/10.1038/ncomms15697, 2017.

o Wada et al.: Human–water interface in hydrological modelling: current status and future directions, Hydrol. Earth Syst. Sci., 21, 4169-4193.

Reply: Thanks for the suggestion. We have revised the sentence following the suggestion.

- P5, L2: I would suggest omitting ‘preliminary’

Reply: Changed.

- P7, L14-17: Showing the individual models in figure S2 makes the figure too busy to read. Why not use the same format as in figure 2 by showing a band around the median. Also, it would be useful to show the same type of figure as figure 2 but for streamflow.

Reply: We have redrawn Figure S2 and added a figure (Figure S3 in the revised manuscript and below) for the simulated and observed annual streamflow following the suggestion.

A brief description has been added.

Revision in the manuscript (Subsection 3.1, the second paragraph (new added)):

The model spreads in the ensembles of seasonal streamflow and the deviations between observation and simulations are relatively larger in the northern basins than those in the southern basins (see Figure S2 for each basin). Comparison between the simulated and observed annual streamflow (Figure S3) shows similar patterns as the seasonal streamflow with respect the discrepancies between northern and southern basins. The Nash-Sutcliffe coefficient was calculated for the multimodel median and observed monthly streamflow at each station (see Table S2), which shows that the multimodel medians have better performance in the southern basins. This evaluation indicates that the multimodel simulations have relatively poor performance in northern basins and most stations with low Nash-Sutcliffe coefficients have smaller streamflow (e.g., in dry areas or upper reaches). The large spreads between models underline the necessity of using ensemble medians rather than individual models for the attribution of streamflow changes.

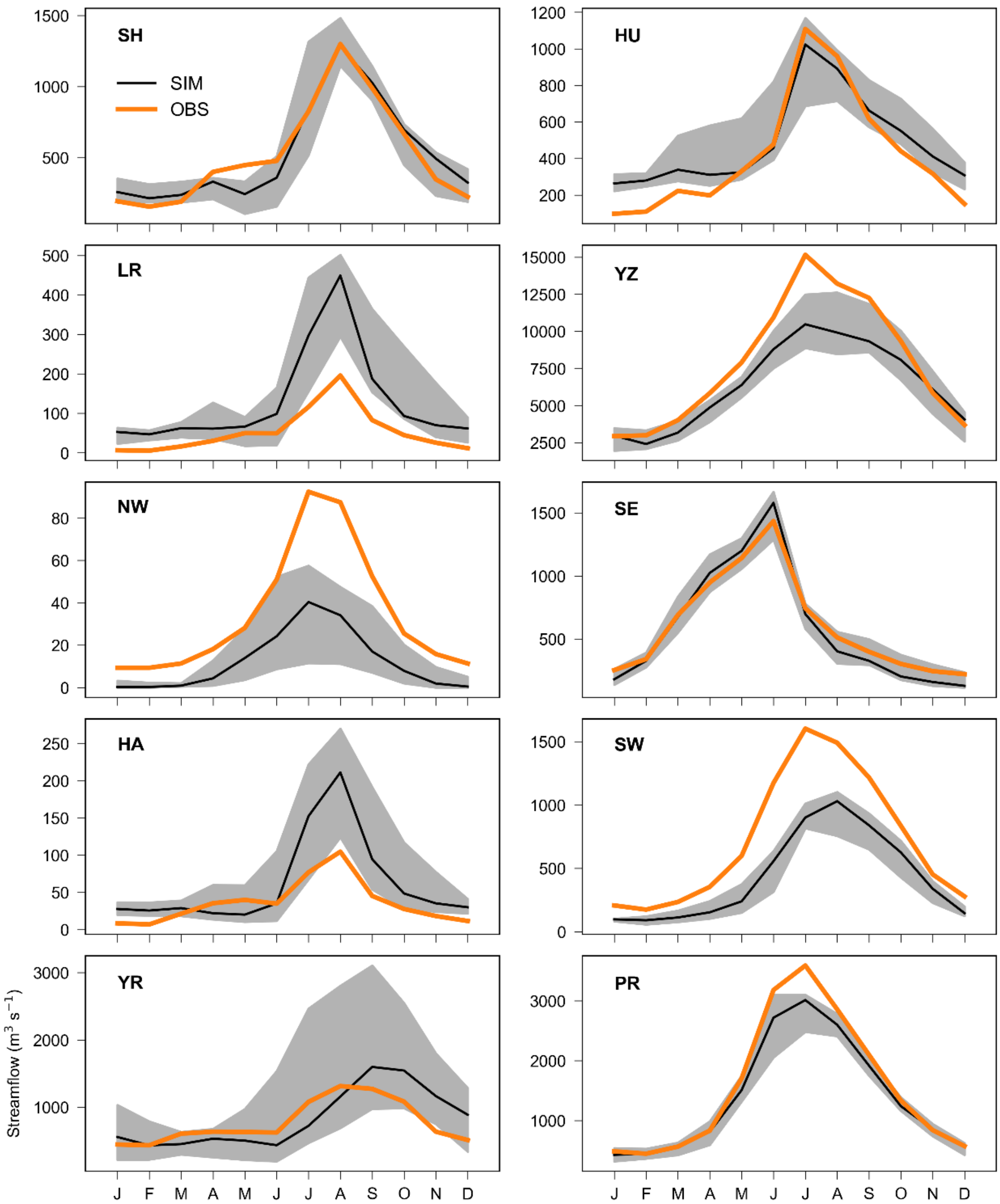

Figure S2. Seasonal cycle of streamflow from observations (orange) and multimodel medians (black). The observations are the average values of the hydrological stations, while the simulations are averaged values over the grid cells identified by the location of stations. The grey areas show the 25th and 75th percentiles of the multimodel simulations. Northern basins: Songhua River (SH), Liao River (LR), Northwest Rivers (NW), Hai River (HA), Yellow River (YR), Huai River (HU); Southern basins: Yangtze River (YZ), Southeast Rivers (SE), Southwest Rivers (SW), Pearl River (PR).

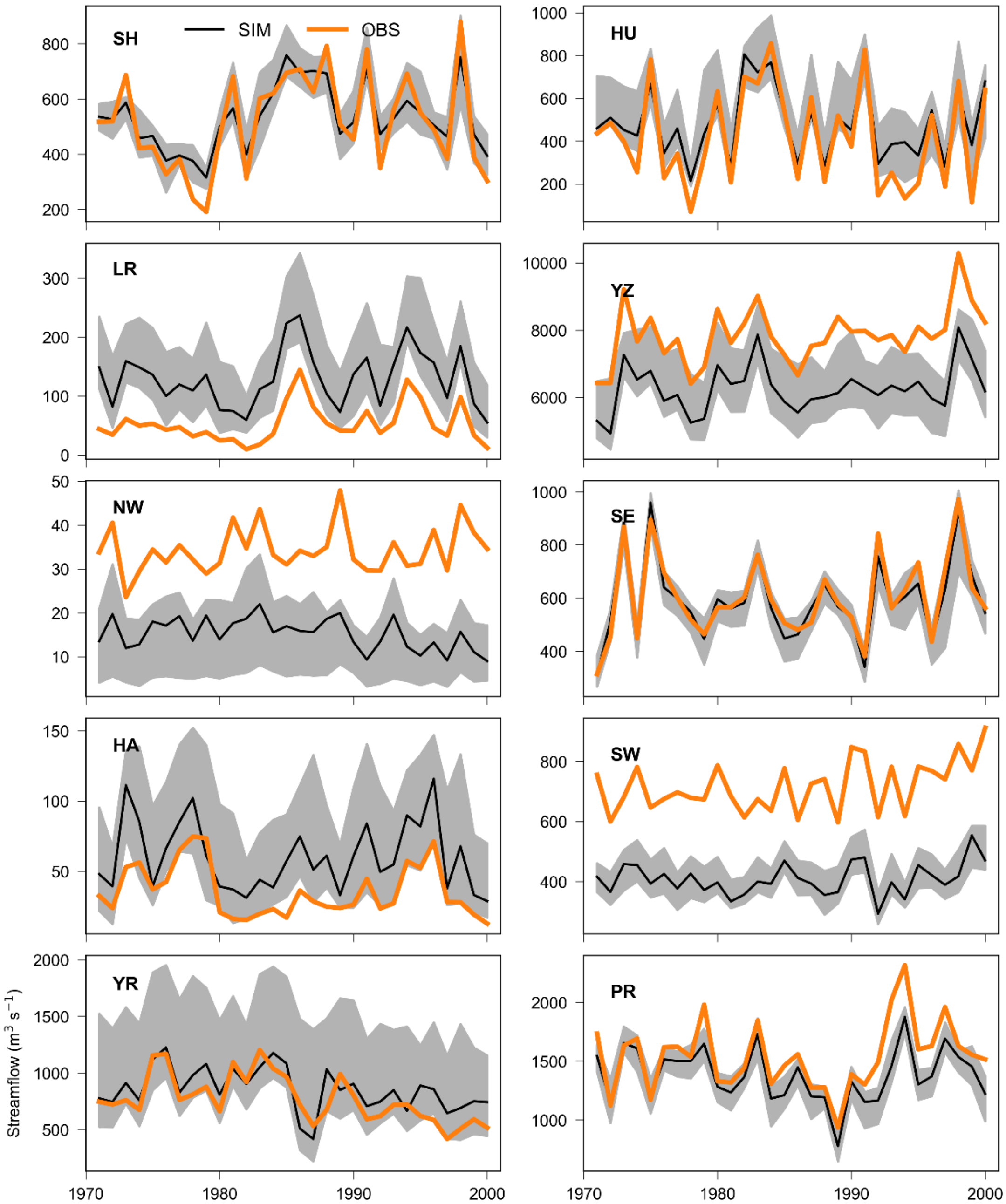

Figure S3. Simulated (black) and observed (orange) mean annual streamflow at the hydrological stations in each basin. The observations are the average values of the hydrological stations, while the simulations are averaged values over the grid cells identified by the location of stations. The grey areas show the 25th and 75th percentiles of the multimodel simulations.

- P7, L18-24: I realize that given the large departures in water withdrawal estimates, matching streamflow gauge observations might be a challenge, unless the authors believe that simulated water withdrawals might be equally or even more reliable than the statistically collected data, which have their own challenges.

Reply: We would not state that the simulations of water withdrawals are equally or more reliable than the statistically collected data. In fact, they are largely based on statistically collected data (e.g., Flörke et al. 2013; Hanasaki et al., 2008). We agree that the large spreads in the multimodel simulations of water withdrawals should be one uncertainty source to the streamflow simulations, but the effect is not superimposing (e.g., Fig. 9 in Müller Schmied et al 2014 for one GHM). On the other hand, Veldkamp et al. (2018) showed that inclusion of human impacts such as water withdrawals leads to better model performances. The simulations of water withdrawals remain a challenge, though great efforts have been made by the community. We have added a statement to address this concern at the end of this paragraph in the revised manuscript, but would not further elaborate it since it is not the focus of this study.

Revision in the manuscript (Subsection 3.1, the last paragraph)

The large deviations in the multimodel simulations of water withdrawals could make the modeling of streamflow more challenging (Döll et al., 2016; Wada et al., 2017).

- P7, L18-24: Are water withdrawals taken from surface water sources or also groundwater sources? What about return flows? Also, I am assuming that glacier melting, which contributes to streamflow, is simulated in these models, but that region is not included in the analysis. I realize that some of these were mentioned in the results, but incorporating some of these details briefly when discussing the method or the results from the evaluation exercise would suffice.

Reply: The sources of water withdrawals are shown in Table S1, depending on models, which may include river channel, reservoirs, groundwater and lakes. Return flows were considered in different ways for different water uses (e.g., Müller Schmied et al., 2014; Wada et al., 2014; Pokhrel et al., 2015). Glacier melting was not simulated in most GHMs (except PCR-GLOBWB) in this study. We have added the absence of glacier melting in the models as a reason for excluding the Tibet plateau region, and described the sources of water withdrawals in the Method section (please see the reply to the 3rd comment of reviewer #1) in the revised manuscript.

Revision in the manuscript (Subsection 2.1, the first paragraph)

The simulations may have large uncertainties over the Tibetan Plateau because long-term meteorological and streamflow observations are sparse in this region (Zhang et al., 2017) *and the modeling of glacier melting is absence in most of the models*.

- P10, L23-29: how does the model specify how much water is taken from surface water vs groundwater sources? Are the small pockets of increased MAF due to human impacts (Fig 5c) attributed to technological change (e.g., irrigation efficiency), or return flow from groundwater pumping, or something else?

Reply: Generally, groundwater is withdrawn when the water use requirement is not met due to limited accessibility to or insufficient quality of surface water. Groundwater withdrawal was considered in most models (see Table S1), but the pumping rate may vary substantially between models (Wada et al., 2016). It is difficult to determine the groundwater pumping rate since groundwater storage is usually unknown. The fraction of groundwater for water use is determined from reported statistics data (Siebert et al., 2010, used in WaterGAP) or estimated in the model (e.g., PCR-GLOBWB, see Wada et al., 2014). We have briefly clarified it in the Method section (also see the reply to the 3rd comment of reviewer #1) in the revised manuscript.

The increased MAF should be mainly due to return flow, but we cannot identify it from which source because of lacking related model output currently. Technological development may improve water use efficiency and reduce the amount of withdrawals. However, it may be not the reason for the slight MAF increase induced by DHI change, because water withdrawal increased over the study period (see Figure 2). We have clarified it in the revised manuscript.

Revision in the manuscript (Subsection 3.4, the first paragraph)

Compared to the first sub-period, in the second sub-period MAF increased by more than 30% in many river segments of the Northwest Rivers and increased by more than 5% in large parts of the Huai River, *which may be due to the return flow from water withdrawals.*

- P11, L7: I would suggest omitting the sentence about the US and Canada. It breaks the flow of the paragraph which is talking specifically about China.

Reply: Removed.

- P13, L14-30: To me this, this is a key contribution of this study. Yes, I agree that the results are not necessarily comparable in term magnitudes due to the highlighted reasons by the authors. But a missing discussion point is to why they fundamentally differ in their findings. I don't agree that either one of these two approaches (small scale using statistical approaches vs large scale modeling similar to this study) is necessarily superior. Each approach has its own pros and cons. So articulating why this approach differs from earlier findings is critical.

Reply: We agree that both the methods has its own pros and cons. At the end of the discussion, we have emphasized the importance of using multiple approach to obtain more reliable assessment. In the revised manuscript, we have rewritten the last paragraph of the discussion, wherein we clearly stated the key difference between the method in previous studies and this study.

Revision in the manuscript (Subsection 4.6, the last paragraph)

One major difference between previous studies (e.g., Li et al., 2007; Bao et al., 2012) and this study is that the former estimates DHI contribution by comparing simulations with observations while we compare two simulation experiments. The former may be subject to uncertainty in comparing the data from two systems (i.e., the model and the real world). In this study, the two simulation experiments favor the estimation of DHI contribution in a consistent manner that is largely free of uncertainty in the data from different systems. The multimodel simulations also allow profiling the uncertainties among models and input forcings, which is *difficult for a single model assessment. However, the deficiency of this approach is that DHI is not real. Therefore, the assessment is inevitably influenced by the extent to which the models can reproduce the real DHI.* Considering the complexity of DHI on streamflow and the ability of current hydrological models in reproducing historical hydrological changes, multimodel simulations and different attribution approaches are well worth obtaining more robust assessments (Liu et al., 2017; Yuan et al., 2018).

Reference:

Bao, Z., J. Zhang, G. Wang, G. Fu, R. He, X. Yan, J. Jin, Y. Liu, and A. Zhang (2012), Attribution for decreasing streamflow of the Haihe River basin, northern China: Climate variability or human activities?, J. Hydrol., 460-461, 117-129, doi: 10.1016/j.jhydrol.2012.06.054.

Döll, P., H. Douville, A. Güntner, H. Müller Schmied, and Y. Wada (2016), Modelling Freshwater Resources at the Global Scale: Challenges and Prospects, Surv. Geophys., 37(2), 195-221, doi: 10.1007/s10712-015-9343-1.

Fader, M., S. Rost, C. Müller, A. Bondeau, and D. Gerten (2010), Virtual water content of temperate cereals and maize: Present and potential future patterns, J. Hydrol., 384(3–4), 218-231, doi: 10.1016/j.jhydrol.2009.12.011.

Flörke, M., E. Kynast, I. Bärlund, S. Eisner, F. Wimmer, and J. Alcamo (2013), Domestic and industrial water uses of the past 60 years as a mirror of socio-economic development: A global simulation study, Global Environ. Change, 23(1), 144-156, doi: 10.1016/j.gloenvcha.2012.10.018.

Hanasaki, N., S. Kanae, T. Oki, K. Masuda, K. Motoya, N. Shirakawa, Y. Shen, and K. Tanaka (2008), An integrated model for the assessment of global water resources – Part 1: Model description and input meteorological forcing, Hydrol. Earth Syst. Sci., 12(4), 1007-1025, doi: 10.5194/hess-12-1007-2008.

Lehner, B., et al. (2011), High-resolution mapping of the world's reservoirs and dams for sustainable river-flow management, Frontiers in Ecology and the Environment, 9(9), 494-502, doi: 10.1890/100125.

Li, L., L. Zhang, H. Wang, J. Wang, J. Yang, D. Jiang, J. Li, and D. Qin (2007), Assessing the impact of climate variability and human activities on streamflow from the Wuding River basin in China, Hydrol. Processes, 21(25), 3485-3491, doi: doi:10.1002/hyp.6485.

Liu, X., Q. Tang, H. Cui, M. Mengfei, D. Gerten, S. Gosling, Y. Masaki, Y. Satoh, and Y. Wada (2017), Multimodel uncertainty changes in simulated river flows induced by human impact parameterizations, Environ. Res. Lett., 12(2), 025009, doi: 10.1088/1748-9326/aa5a3a.

Masaki, Y., N. Hanasaki, H. Biemans, H. Müller Schmied, Q. Tang, Y. Wada, S. N. Gosling, K. Takahashi, and Y. Hijioka (2017), Intercomparison of global river discharge simulations focusing on dam operation—multiple models analysis in two case-study river basins, Missouri–Mississippi and Green–Colorado, Environ. Res. Lett., 12(5), 055002.

Müller Schmied, H., S. Eisner, D. Franz, M. Wattenbach, F. T. Portmann, M. Flörke, and P. Döll (2014), Sensitivity of simulated global-scale freshwater fluxes and storages to input data,

hydrological model structure, human water use and calibration, Hydrol. Earth Syst. Sci., 18(9), 3511-3538, doi: 10.5194/hess-18-3511-2014.
Pokhrel, Y. N., S. Koirala, P. J. F. Yeh, N. Hanasaki, L. Longuevergne, S. Kanae, and T. Oki (2015), Incorporation of groundwater pumping in a global Land Surface Model with the representation of human impacts, Water Resour. Res., 51(1), 78-96, doi: 10.1002/2014WR015602.
Portmann, F. T., S. Siebert, and P. Döll (2010), MIRCA2000—Global monthly irrigated and rainfed crop areas around the year 2000: A new high-resolution data set for agricultural and hydrological modeling, Global Biogeochem. Cycles, 24(1), GB1011, doi: 10.1029/2008GB003435.
Siebert, S., J. Burke, J. M. Faures, K. Frenken, J. Hoogeveen, P. Döll, and F. T. Portmann (2010), Groundwater use for irrigation – a global inventory, Hydrol. Earth Syst. Sci., 14(10), 1863-1880, doi: 10.5194/hess-14-1863-2010.
Veldkamp, T. I. E., et al. (2018), Human impact parameterizations in global hydrological models improve estimates of monthly discharges and hydrological extremes: a multi-model validation study, Environ. Res. Lett., 13(5), 055008, doi: 10.1088/1748-9326/aab96f.
Wada, Y. (2016), Modeling Groundwater Depletion at Regional and Global Scales: Present State and Future Prospects, Surv. Geophys., 37(2), 419-451, doi: 10.1007/s10712-015-9347-x.
Wada, Y., D. Wisser, and M. F. P. Bierkens (2014), Global modeling of withdrawal, allocation and consumptive use of surface water and groundwater resources, Earth Syst. Dynam., 5(1), 15-40, doi: 10.5194/esd-5-15-2014.
Wada, Y., et al. (2017), Human–water interface in hydrological modelling: current status and future directions, Hydrol. Earth Syst. Sci., 21(8), 4169-4193, doi: 10.5194/hess-21-4169-2017.
Yin, Y., Q. Tang, X. Liu, and X. Zhang (2017), Water scarcity under various socio-economic pathways and its potential effects on food production in the Yellow River basin, Hydrol. Earth Syst. Sci., 21(2), 791-804, doi: 10.5194/hess-21-791-2017.
Yuan, X., Y. Jiao, D. Yang, and H. Lei (2018), Reconciling the attribution of changes in streamflow extremes from a hydroclimate perspective, Water Resour. Res., doi: doi:10.1029/2018WR022714.
Zhang, C., Q. Tang, and D. Chen (2017), Recent Changes in the Moisture Source of Precipitation over the Tibetan Plateau, J. Climate, 30(5), 1807-1819, doi: 10.1175/jcli-d-15-0842.1.

Multimodel assessments of human and climate impacts on mean annual streamflow in China

Xingcai Liu[1,2], Wenfeng Liu[2,3], Hong Yang[2,4], Qiuhong Tang[1,5], Martina Flörke[6], Yoshimitsu Masaki[7], Hannes Müller Schmied[8,9], Sebastian Ostberg[10], Yadu Pokhrel[11], Yusuke Satoh[12,13], Yoshihide Wada[12]

[1]Key Laboratory of Water Cycle and Related Land Surface Processes, Institute of Geographic Sciences and Natural Resources Research, Chinese Academy of Sciences, A11, Datun Road, Chaoyang District, Beijing, China
[2]Eawag, Swiss Federal Institute of Aquatic Science and Technology, Ueberlandstrasse 133, CH-8600 Duebendorf, Switzerland
[3]Laboratoire des Sciences du Climat et de l'Environnement, LSCE/IPSL, CEA-CNRS-UVSQ, Université Paris-Saclay, F-91191 Gif-sur-Yvette, France
[4]Department of Environmental Sciences, MGU, University of Basel, Petersplatz 1, CH-4003 Basel, Switzerland
[5]College of Resources and Environment, University of Chinese Academy of Sciences, Beijing 100049, China
[6]Center for Environmental Systems Research, University of Kassel, Kassel, Germany
[7]Graduate School of Science and Technology, Hirosaki University, Hirosaki, Japan
[8]Institute of Physical Geography, Goethe-University Frankfurt, Altenhöferallee 1, 60438 Frankfurt, Germany
[9]Senckenberg Biodiversity and Climate Research Centre (SBiK-F), Senckenberganlage 25, 60325 Frankfurt, Germany
[10]Earth System Analysis, Potsdam Institute for Climate Impact Research (PIK), Potsdam, Germany
[11]Department of Civil and Environmental Engineering, Michigan State University, East Lansing, MI 48824 United States of America
[12]International Institute for Applied Systems Analysis, Laxenburg, Austria
[13]National Institute for Environmental Study, Tsukuba, Japan

Correspondence to: Qiuhong Tang (tangqh@igsnrr.ac.cn)

Abstract. Human activities, as well as climate ~~change~~variability, have had increasing impacts on natural hydrological systems, particularly streamflow. However, quantitative assessments of these impacts are lacking on large scales. In this study, we use the simulations from six global hydrological models driven by three meteorological forcings to investigate direct human impact (DHI) and climate ~~change~~ impact on streamflow in China. Results show that, in the sub-periods of 1971-1990 and 1991-2010, one-fifth to one-third of mean annual streamflow (MAF) reduced due to DHI in northern basins and much smaller (< 4%) MAF reduced in southern basins. From 1971-1990 to 1991-2010, total MAF changes range from -13% to 10% across basins, wherein the relative contributions of DHI change and climate ~~change~~ variability show distinct spatial patterns. DHI change caused decreases in MAF in 70% of river segments, but climate ~~change~~ variability dominated the total MAF changes in 88% of river segments of China. In most northern basins, climate ~~change~~ variability results in changes of -9% to 18% of MAF, while DHI change results in decreases of 2% to 8% in MAF. In contrast with the climate variability~~impacts of climate change~~ that may increase or decrease streamflow, DHI change almost always contributes to decreases in MAF over time, wherein water withdrawals are supposed to be the major impact on streamflow. This quantitative assessment can be a reference for attribution of streamflow changes at large scales

despite uncertainty remains. We highlight the significant DHI in northern basins and the necessity to modulate DHI through improved water management towards a better adaptation to future climate change.
Keywords: streamflow; human impact; multimodel simulation; ISIMIP2a; China

1 Introduction

Human activities have remarkably intensified and significantly altered hydrological regimes and water resources worldwide (Oki and Kanae, 2006; Döll et al. 2009; Tang and Oki, 2016). They have been reported to have aggravated hydrological drought and impaired hydrological resilience in many regions (Wada et al., 2013; Wada and Heinrich, 2013; Veldkamp et al., 2017). Human impact (here we only consider the direct human impact (DHI), e.g., that caused by the construction and management of dams and reservoirs, water withdrawal from surface water, and groundwater pumping, etc.) on streamflow has been on the rise across the world (Jaramillo and Destouni, 2015), causing the same order of magnitude of hydrologic alterations as by climate change/variability in some regions (Ian and Reed, 2012; Haddeland et al., 2014; Zhou et al., 2015). As such, there has been increased attention in attributing hydrological impacts from various drivers (Patterson et al., 2013; Tan and Gan, 2015; Bosmans et al., 2017). Understanding the relative contributions of DHI to streamflow changes is of great importance for climate change adaptation and sustainable development (Yin et al., 2017).

In China, the hydrological system is experiencing significant changes induced by both climate ~~change~~ and human ~~activities~~ impacts (Piao et al., 2010; Tang et al., 2013; Liu et al., 2014; Wada et al., 2017). Great efforts have been made to quantify the relative contributions of DHI in China (Liu and Du, 2017). Some studies have shown that DHI outweighed climatic impact on streamflow / runoff in several small catchments in the Hai River (Wang et al., 2009; Wang et al., 2013b) and the Yellow River (Li et al., 2007; Tang et al., 2008; Zhan et al., 2014; Chang et al., 2016). Other studies have reported that the construction and operation of the Three Gorges Reservoir resulted in considerable changes in streamflow (Wang et al., 2013a) but DHI contributed to small changes in streamflow in some catchments (Liu et al., 2012; Ye et al., 2013) and slight changes in lake areas in the Yangtze River basin (Wang et al., 2017). Most of these studies attributed human impact by comparing observed streamflow to simulations which were estimated with a climate elasticity approach based on the Budyko framework (Zhang et al., 2001) or with hydrological models (Wang et al., 2009; Wang et al., 2010; Yuan et al., 2018). These assessments largely relied on hydroclimatic observations and were performed on relatively small catchment scales to obtain quantitatively distinguishable attributions. The previous studies assessed DHI on streamflow changes at the outlets of catchments, but the spatial extents of the impacts have not been adequately examined. As mentioned above, many previous studies reported large DHI on streamflow; however, a recent large-scale assessment over the United States and Canada showed that human activities such as water management did not substantially alter the hydrological effects of climate change (Ficklin et al., 2018). In addition, the potential uncertainty associated with DHI and streamflow simulations can hardly be estimated from a single model assessment as done in previous studies. Therefore, an improved assessment with larger spatial coverage and by employing a multimodel comparison approach is essential to understand regional difference and associated uncertainty of the impacts.

The recent development of human impact parameterizations in hydrological models has facilitated the assessment of the DHI on streamflow (Pokhrel et al., 2016; Liu et al., 2017b; Veldkamp et al, 2018). Consequently, several global hydrological modelling initiatives considering human impact have been undertaken, e.g., by the Inter-Sectoral Impact Model Intercomparison Project phase 2a (ISIMIP2a, Gosling et al., 2017). Under the ISIMIP2a framework, retrospective simulations of hydrological changes were performed for both natural conditions and those with human activities by six global hydrological models (GHMs). The simulations provide a basis for quantifying the streamflow changes caused by various drivers in a consistent manner on large scales. Meanwhile, the grid-based simulations allow an attribution at different geographic levels and, therefore, provide more detail information about regional streamflow changes. The ISIMIP2a simulations have included the most important DHI over large scales including the operation of reservoirs/dams on rivers as well as sectoral water withdrawals for irrigation, industry, domestic, and livestock. In this study, using the ISIMIP2a multimodel simulations, we quantify the relative contribution of DHI and climate change variability on streamflow changes in the major river basins in China at decadal timescale during the 1971-2010 period. This is the first study to focus on performing such a quantitative assessment for all rivers of China with comparable modeling experiments. This study can serve as a reference for attribution of streamflow changes at large scales that can facilitate regional water resources management under climate change and growing human impact on freshwater system.

2 Method and data

2.1 Simulation data

In this study, we use the simulations of monthly streamflow of China produced by six GHMs, namely, DBH (Tang et al., 2007, 2008; Liu et al., 2016), H08 (Hanasaki et al., 2008a, 2008b), LPJmL (Bondeau et al. 2007; Rost et al. 2008; Biemans et al. 2011; Schaphoff et al. 2013), MATSIRO (Takata et al., 2003; Pokhrel et al., 2015), PCR-GLOBWB (Wada et al., 2014), WaterGAP2 (Flörke et al., 2013; Müller Schmied et al., 2014, 2016). Two experiments, i.e., simulations with (VARSOC) and without (NOSOC) human impact, were performed at a half-degree spatial resolution for the 1971-2010 period by using the six GHMs following the ISIMIP2a simulation protocol (https://www.isimip.org/protocol/#isimip2a). All the model runs used the same river routing map (DDM30, Döll and Lehner, 2002). Human impact considered in the VARSOC experiment (see the maps in Figure S1 and Table S1 for more details) include the time-varying areas for both irrigated and rainfed cropland (Fader et al., 2010; Portmann et al., 2010) and reservoirs (dams) from the Global Reservoir and Dam (GRanD) Database (Lehner et al., 2011) including their commissioning year (see Figure S1 and Table S1 for more detail). Reservoir regulation was considered in the VARSOC experiment, which often reduces high streamflow in high-flow seasons and increases streamflow in dry seasons (Masaki, et al., 2017). Inter-basin water transfer was not considered in any of the model runs. For both experiments, the GHMs were forced by three global meteorological forcing products (GMFs), i.e., the PGMFD v.2 (Princeton) (Sheffield et al., 2006), GSWP3 (http://hydro.iis.u-tokyo.ac.jp/GSWP3/), and a combination of WFD (until 1978, Weedon et al., 2011) and WFDEI (from 1979 onwards, Weedon et al., 2014) datasets. Ensembles of annual streamflow are derived from the simulations of NOSOC (referred to as Q_n) and VARSOC (referred to as Q_v) experiments, respectively, for river segments (here a grid cell is treated as a river segment regardless of the cases that a grid cell contains several small river segments) which are then spatially averaged for individual basins. Long-term mean annual streamflow (MAF) in each river segment is calculated for both NOSOC and VARSOC simulations over a specific period (see section 2.3) and then is spatially-averaged over individual basins for each ensemble member. In addition to streamflow, total runoff from NOSOC and VARSOC simulations and water withdrawals from VARSOC simulations are also derived at grid cells and individual basins for associated analyses. The simulations may have large uncertainties over the Tibetan Plateau because long-term meteorological and streamflow observations are sparse in this region (Zhang et al., 2017) and the modeling of glacier melting is absence in most of the models. Therefore, the simulation data in the Tibetan Plateau region are removed and are not included in spatial averages by masking the grid cells with altitudes higher than 4000 meters in all analyses.

Human impact considered in the VARSOC experiment (see the maps in Figure S1 and Table S1 for more details) includes the time-varying areas for both irrigated and rainfed cropland (Fader et al., 2010; Portmann et al., 2010) and reservoirs (dams) from the Global Reservoir and Dam (GRanD) Database (Lehner et al., 2011) including their commissioning year (see Figure S1 and Table S1 for more detail). Reservoir regulation was considered in the VARSOC experiment, which often reduces high streamflow in high-flow seasons and increases streamflow in dry seasons (Masaki, et al., 2017). -Inter-basin water transfer was not considered in any of the model runs. The simulations of water withdrawals are different between the GHMs with respect to water use requirements and water withdrawal sources which are shown in Table S1. The sources of water withdrawals, depending on models, may include river channel, reservoirs, groundwater and lakes, and their fractions may be determined from reported statistics (e.g., Siebert et al., 2010) or estimated in models (Wada et al., 2014). In addition to the irrigation water requirement which is usually estimated by coupling crop models, most GHMs considered the requirements for domestic and industrial water use which were prescribed in H08 (Hanasaki et al., 2008), LPJmL and MATSIRO (Pokhrel et al., 2015) or were estimated according to the population, socioeconomic and technological development in PCR-GLOBWB (Wada et al., 2014) and the population, thermal electricity production, gross added value, and technological change in WaterGAP (Flörke et al., 2013). Water use requirement for livestock was also prescribed in the LPJmL model, and estimated according to livestock densities in PCR-GLOBWB and WaterGAP2.

2.2 Observed monthly streamflow and reported water withdrawals

The ISIMIP2a streamflow simulations have been extensively validated with observations over the world in several studies (Liu et al, 2017b; Veldkamp et al., 2018; Zaherpour et al., 2018), but were not fully evaluated in China due to limited observations, particularly for the water withdrawals. Therefore, before the quantitative attribution, an ~~preliminary~~ evaluation of the multimodel simulations is performed, which may add confidence regarding the GHMs' performance over China. Observations of monthly streamflow from 44 hydrological stations in China (Figure 1) during 1971-2000 are used for model validation. The observations since 2001 are not available in this study. Some stations are relocated on the map to reconcile the catchment areas of the stations and the accumulative flow areas of corresponding gird cells from the DDM30 river network. After relocation, the differences are mostly less than 10% (about 50% at 5 stations) between the reported catchment areas of stations and the accumulative flow areas from the DDM30 river network. Annual water withdrawals in individual basins for the years of 1980, 1985, 1990, 1995, and 1997-2010 were collected from China Water Resources Bulletin from the Ministry of Water Resources (MWR) of China (http://www.mwr.gov.cn/sj/tjgb/szygb/).

2.3 Streamflow changes and attribution

The study period is evenly split into two sub-periods (P1 for 1971-1990 and P2 for 1991-2010). The DHI-induced MAF changes over time is calculated as:

$$\begin{cases} Q_h^{P1} = 100 \times \frac{Q_v^{P1} - Q_n^{P1}}{Q_n^{P1}} \\ Q_h^{P2} = 100 \times \frac{Q_v^{P2} - Q_n^{P2},}{Q_n^{P2}} \end{cases} \quad (1)$$

where Q_h^{P1} and Q_h^{P2} denote MAF changes (%) induced by DHI during the sub-periods P1 and P2, respectively; Q_v^{P1} and Q_v^{P2} denote MAF from the VARSOC experiment for the two sub-periods, respectively; Q_n^{P1} and Q_n^{P2} denote MAF from the NOSOC experiment for the two sub-periods, respectively.

The contribution of *DHI change* (corresponding to *climate ~~change~~variability*) on streamflow changes between the two sub-periods is also examined. MAF difference between the two periods in the VARSOC experiment is defined as the total MAF changes (ΔQ_a) caused by both climate ~~change~~ variability and DHI change from P1 to P2, which is expressed as a percentage of the MAF of the first sub-period P1:

$$\Delta Q_a = 100 \times \frac{Q_v^{P2} - Q_v^{P1}}{Q_v^{P1}}. \quad (2)$$

The difference between the two periods in the NOSOC experiment is defined as streamflow changes induced by only climate variability ~~change~~ (ΔQ_c) and expressed as a percentage of Q_v^{P1} in order to be comparable with ΔQ_a:

$$\Delta Q_c = 100 \times \frac{Q_n^{P2} - Q_n^{P1}}{Q_v^{P1}}. \quad (3)$$

The difference between ΔQ_a and ΔQ_c then counts as MAF changes induced by DHI change (ΔQ_h) between the two sub-periods:

$$\Delta Q_h = \Delta Q_a - \Delta Q_c = 100 \times \frac{(Q_v^{P2} - Q_v^{P1}) - (Q_n^{P2} - Q_n^{P1})}{Q_v^{P1}}. \quad (4)$$

Unless otherwise stated, ΔQ_a, ΔQ_c, ΔQ_h are relative changes (%) with respect to Q_v^{P1} in this paper.

To address the potential uncertainty resulting from the use of sub-periods, similar analyses are performed for three different sub-periods, namely, 1981-1990, 1991-2000, and 2001-2010, with comparison to the sub-period 1971-1980. For these analyses, MAF is calculated over each decade.

In addition to streamflow, changes in water withdrawals and total runoff between the two sup-periods are also analyzed to explore their links with MAF changes.

2.4 Multimodel ensemble

Ensemble medians across the 18 GHM-GMF combinations (6 GHMs and 3 GMFs) are used for analyses of streamflow and runoff. But 12 ensemble members are used for water withdrawals because only 4 GHMs (H08, LPJmL, PCR-GLOBWB, and MATSIRO) provide related output for the ISIMIP2a simulations. The interquartile range (IQR), i.e., the range between 25th and 75th percentiles, is calculated to present the spread across multimodel ensembles. The ratio of IQR to the median is used to measure the uncertainty in multimodel simulations of streamflow, which is comparable across regions.

3 Results

3.1 Evaluation of multimodel simulations

In this study, the northern basins refer to Songhua River (SH), Liao River (LR), Northwest Rivers (NW), Hai River (HA), Yellow River (YR), Huai River (HU); and the southern basins refer to the Yangtze River (YZ), Southeast Rivers (SE), Southwest Rivers (SW), Pearl River (PR) (Figure 1). The ensemble medians of MAF at grid cells over the 1971-2000 period from the VARSOC experiment show distinct spatial pattern of high streamflow in southern basins and relatively low streamflow in northern basins (Figure 1). The multimodel simulations show larger spreads in the northern basins. The ratios of IQR/median are larger than 1 or 2 in the Northwest basin, the Yellow River basin and Liao River basin. Smaller spread (IQR/median less than 0.5) is found in the middle and lower reaches of the Yangtze River basin, the Pearl River basin, and the Southeast basin.

The inner plot shows the comparison between observed seasonal streamflow averaged across all hydrological stations and the averaged simulations in all river segments identified by stations over the 1971-2000 period. The ensemble medians of seasonal cycle generally coincide with the observations. However, there are large variations across all model ensembles with some of them deviating from observations. It should be noted that the stations are located at different reaches of individual basins. Thus, the station-averaged ~~seasonality~~ estimates are~~is~~ largely dominated by those with large streamflow (e.g., at the lower reaches). Additionally, the coverage of stations used is relatively small (due to data availability), especially in hydrologically variable regions like in the Northwest Rivers, leading to not necessarily representative evaluation of the performance of the GHMs in the whole basin. The model spreads in the ensembles of seasonal streamflow in the northern basins are ~~usually~~ relatively larger than those in the southern basins (see Figure S2 for each basin), which underlines the necessity of using ensemble medians rather than individual models for the attribution of streamflow changes. Comparison between the simulated and observed annual streamflow (Figure S3) shows similar patterns as the seasonal streamflow with respect the discrepancies between northern and southern basins. The Nash-Sutcliffe coefficient was calculated for the multimodel median and observed monthly streamflow at each station (see Table S2), which shows that the multimodel medians have better performance in the southern basins. This evaluation indicates that the multimodel simulations have relatively poor performance in northern basins and most stations with low Nash-Sutcliffe coefficients have smaller streamflow (e.g., in dry areas or upper reaches). The large spreads between models underline the necessity of using ensemble medians rather than individual models for the attribution of streamflow changes.

Compared to the reported data by the Ministry of Water Resources (MWR) of China, the ensemble medians from ISIMIP2a simulations underestimated water withdrawals in most northern basins except for the Yellow River (Figure 2). The simulations underestimate water withdrawals by more than 50% in the Northwest Rivers and the Hai River and by more than 30% in the Songhua River and Liao River. The simulated water withdrawals are 12% less than reported data in the Huai River. In the Yellow River and the Southeast Rivers, water withdrawals are overestimated by 20% or more. The overestimation of water withdrawals is the largest (80%) in the Southwest Rivers. Small differences between simulations and reported data are found in the Yangtze River (-1%) and the Pearl River (-6%). The large deviations in the multimodel simulations of water withdrawals could make the modeling of streamflow more challenging (Döll et al., 2016; Wada et al., 2017).

3.2 Annual streamflow and DHI-induced streamflow change

Figure 3 shows the spatially averaged ensemble medians of Q_n and Q_v over China, the northern and southern basins. Q_n and Q_v show considerable annual variations and no statistically significant trends over the 1971-2010 period. The relative differences between Q_n and Q_v over China range from -8% to -4% and show a statistically significant downward trend over the study period (Figure 3a). The differences between Q_n and Q_v over the northern basins are larger than those for the southern basins. The absolute differences (not shown here) are -37 to -14 (m^3/s) for the northern basins and are -37 to -7 (m^3/s) for the southern basins. The relative differences for the northern basins (Figure 3b) are also larger than those for the southern basins (Figure 3c). The former ranges from -30% to -10% while the latter ranges from -4% to -1%. Statistically significant downward trend is found in the relative differences for the northern basins, while non-significant downward trend is found for the southern basins. The downward trend in the differences indicates that annual streamflow has been increasingly affected by human impact.

3.3 MAF altered by DHI in the two sub-periods

Considerable decreases in long-term MAF are induced by DHI in the two sub-periods (Figure 4a and 4b for Q_h^{P1} and Q_h^{P2}, respectively) in most northern basins. About 3% and 4% of total river segments in China show large negative values (i.e., less than -30%) of Q_h^{P1} and Q_h^{P2}, respectively, which are mostly found in some parts of the Northwest Rivers, and the North China Plain. Q_h^{P1} and Q_h^{P2} are negative for more than 90% of the river segments and range from -5% to 0 in more than 60% of the river segments of China. The magnitudes of the basin-averaged Q_h^{P1} and Q_h^{P2} are larger than 10% in northern basins except for the Songhua River (Figure 4c). The magnitudes of Q_h^{P2} are larger than Q_h^{P1} for all basins, especially in the Yellow River. The Northwest Rivers show the largest negative values of Q_h^{P1} and Q_h^{P2} (-31.6% and -33.5%, respectively), which is followed by the Hai River (-24% and -25%), the Yellow River (-17% and -21%) and the Huai River (-17% and -19%). DHI induced slight decreases in MAF (-3.4% to -0.3%) in the southern basins. Overall, DHI altered MAF by -4.4% and -5.6% in China during the sub-periods P1 and P2, respectively.

3.4 MAF changes induced by DHI change and climate variability ~~change~~ between the two sub-periods

The MAF changes induced by DHI change and climate variability ~~change~~ between the two sub-periods are shown in Figure 5. In general, total MAF changes (ΔQ_a, Figure 5a) are larger in northern basins except the Songhua River than in southern basins. Compared to the first sub-period, in the second sub-period MAF increased by more than 30% in many river segments of the Northwest Rivers and increased by more than 5% in large parts of the Huai River, which may be due to the return flow from water withdrawals. MAF increases are also found in considerable areas of southern basins such as the Yangtze River and the Southwest Rivers. MAF decreases are found in most river segments in the Yellow River, the Hai River, and the Liao River. Significant negative values of ΔQ_a (less than -20%) are found in some river segments in the upper reaches of the Southwest Rivers and some parts of the Northwest Rivers. The total MAF decreased by more than 10% (ΔQ_a < -10%) and increased by more than 10% (ΔQ_a > 10%) in about 24% and 17% of river segments of China, respectively.

MAF changes induced by climate variability ~~change~~ between the two sub-periods (ΔQ_c, Figure 5b) have very similar spatial patterns as ΔQ_a (Figure 5a). It indicates that climate ~~change~~ impact dominates MAF changes during the two sub-periods. The magnitudes of ΔQ_c are relatively smaller than those of ΔQ_a in the Hai River and the Yellow River but are larger in the north-western parts of the Northwest Rivers. MAF changes induced by DHI change (ΔQ_h, Figure 5c) are generally large and negative in northern basins. Larger than 10% decrease in MAF induced by DHI is found in some segments of the Northwest Rivers and the lower reaches of the Huai River, the Hai River, and the Liao River. Positive values of ΔQ_h are small and are mostly found in southern river segments. Climate ~~change~~ impact dominated MAF changes in most river segments (88%) of China (Figure 5d). Only 12% of river segments show MAF changes that are mainly caused by DHI change, which are mostly in the northern basins.

MAF changes induced by climate variability ~~change~~ (ΔQ_c) versus those induced by DHI change (ΔQ_h) for all river segments are shown in Figure 6a. Note that very few river segments with values of ΔQ_c (0.9% of total river segments) and ΔQ_h (0.4%) beyond [-100, 100] are not shown in the figure. Magnitudes of ΔQ_c are much larger than those of ΔQ_h. The latter ranges -5% to 5% in most (~ 81%) river segments. ΔQ_h is less than -10% in only about 7% of river segments of China, while even fewer

(~ 3%) segments show ΔQ_h larger than 5%. The values of ΔQ_c range from -10% to 10% in more than half of river segments and range from -20% to 20% in nearly 80% of river segments (see Table S2 S3 for related numbers). ΔQ_h is negative in 70% of river segments, while negative values of ΔQ_c are found in more than half of the river segments of China (see the percentage numbers in Figure 6a and Table S2S3).

The total MAF spatially-averaged over China decreased by only 1% from the first sub-period to second sub-period (Figure 6b; also see Table S3S4-S5 S6 for more details of spatially aggregated ensemble members and medians of ΔQ_a, ΔQ_c, and ΔQ_h in basins). At the basin scale, the magnitudes of MAF changes are usually very small (less than 2%) in southern basins and are relatively large in northern basins (5% to 13%). ΔQ_a in the Hai River shows the largest decrease of 13%, which is followed by nearly 10% decrease in the Yellow River and a 7% decrease in the Liao River. Increases of total MAF are found in the Northwest Rivers (10%), and the Huai River (1.8%) and the Pearl River (1.3%) and the Southwest Rivers (1.2%), which are consistent with the spatial patterns shown in Figure 5a. DHI change causes decreases in MAF (negative ΔQ_h) in all the basins, resulting in a larger decrease or a smaller increase in ΔQ_a compared to ΔQ_c. The largest negative values of ΔQ_h are found in the Northwest Rivers (-8%), the Huai River (-5.4%), and the Hai River (-4.6%, see Table S3S4-S5S6). ΔQ_h is about -2.6% for the Liao River and the Yellow River. ΔQ_h is only about -0.7% to -0.07% in southern basins. The increase of MAF induced by climate variability change (ΔQ_c) are the largest in the Northwest Rivers (18%), followed by the Huai River (6%) and the Pearl River (1%), and climate variability change caused nearly 9% decrease in MAF in the Hai River and the Yellow River.

3.5 Water withdrawal and its changes between the two sub-periods

For both sub-periods, the estimates of long-term mean annual water withdrawals are large (more than 100×10^6 m^3 per year) in many areas of the Huai River, the Hai River and the Yellow River (Figure 7a). Large water withdrawals are also found in some lower reaches of the Yangtze River. In these regions, mean annual water withdrawals are usually larger in the lower reaches compared to the upper reaches, and significantly increased from 1971-1990 to 1991-2010. The relative changes in water withdrawals between the two sub-periods show distinct spatial patterns from northern to southern basins, and generally increased at all river segments of China (Figure 7c). The spatial patterns of changes in water withdrawals resemble those of ΔQ_h, with large values in the Huai River, the Hai River, and the Yellow River, but are relatively smaller in the Northwest Rivers. Similar analysis is performed for changes in total runoff to examine its linkage with streamflow changes. The spatial patterns of changes in total runoff induced by DHI change between the two sub-periods (Figure 7d) are different from that of ΔQ_h (Figure 5c). Total runoff changes are positive in most areas of China due to increasing irrigation water (from both local and external sources) which partly becomes return flow, especially in the Northwest Rivers. Large changes are also found in upper and middle reaches in the Yellow River, the Liao River and the Hai River. The change magnitudes are less than the those induced by climate variability change (not shown here), which is similar as Figure 5d. This indicates that the runoff changes are less linked to streamflow changes in the study period.

4 Discussion

The simulated streamflow in China from the ISIMIP2a VARSOC experiment (i.e., simulations with consideration of DHI) is validated against observed streamflow from 44 hydrological stations. While the multimodel ensemble medians match well with observations, the evaluation indicates that the individual simulations of streamflow are subject to considerable uncertainties among models which are especially pronounced in northern basins as indicated by the ratio of interquartile range to median. The simulations of water withdrawals show large deviations from the reported data in many basins, which partly affects the performance of GHMs in streamflow simulations. It should be noted that the over/underestimation of streamflow at these stations do not necessarily indicates the performance of GHMs in the whole basins because of limited stations used in this study.

Simulated annual streamflow has been increasingly affected by human impact, which is more significant in northern basins. Using the multimodel ensemble medians of streamflow, we quantify the DHI on the long-term MAF during two sub-periods 1971-1990 and 1991-2010, and the long-term MAF changes induced by changes in DHI and climate between the two sub-periods. DHI often results in decreased streamflow in China, particularly in northern rivers, through water withdrawals, while results in increased runoff due to return flow from irrigation. Potential implications of the distinct spatial patterns of DHI and its change on streamflow and the associated uncertainties in current assessment are discussed as follows.

4.1 DHI considerably altered streamflow in northern basins

DHI causes MAF decreases in both of the sub-periods. At the basin level, DHI resulted in decreases by one-fifth to one-third of the long-term MAF based on Q_n in northern basins and slightly altered MAF in southern basins of China. The spatial patterns of the MAF altered by DHI (Q_h) are generally in accordance to those reported by previous studies (Liu and Du, 2017) and are very close to those of irrigated areas of China (see Figure S1). The expansion of agriculture and enhanced irrigation and food demands should be the main reason for the large DHI on streamflow in northern basins (Liu et al. 2015; also see Figure S1c), where agricultural water use accounts for about 70%-90% of total water use as reported by China Water Resources Bulletin from 1997 to 2010. Water withdrawal for irrigation is less due to the large streamflow and relatively wetter conditions in southern basins. Limited water resources can further amplify the effects of damming on river segments in northern basins (Yang and Lu, 2014) despite the fewer reservoirs therein compared to southern basins (see Figure S1a).

4.2 Hydrological effects from DHI change are limited compared with climate variability~~change~~

Though MAF changes between the two sub-periods are relatively small, especially in southern basins, the respective contributions of climate variability ~~change~~ and DHI change are still distinguishable. In general, streamflow changes are dominated by climate variability ~~change~~ between the two sub-periods in most river segments of China. ~~Similar results have been reported by a recent study in the United States and Canada (Ficklin et al., 2018).~~ The small portion (12%) of river segments where DHI change outweighs climate ~~change~~ impact on MAF changes are mostly in northern China. The small magnitudes of MAF changes induced by DHI change between the two sub-periods may be partly due to that DHI change is not significant in most areas of China in the VARSOC experiment. Although the irrigated areas in both the northern and southern basins increased by about 20% in the second sub-period (see Figure S1c), the changes between the two sub-periods are small (less than 5%) in many areas except in the Huai River and the Hai River (see Figure S1b). Furthermore, there are only a few reservoir data from the GRanD database after the year 2000, and most reservoirs in China were built in the first sub-period (see Figure S1d). The reservoirs lacking construction years were set to be built (and operated) at the beginning of the experiment in the model runs.

It is noted that the absolute MAF changes between the two sub-periods are large in main streams in both southern and northern basins (see Figure S3S4); and the significant MAF changes induced by DHI change in the Yangtze River are associated with the large reservoir regulations, e.g., the Three Gorges Reservoir (Wang et al., 2013a).

4.3 Water withdrawals are identified as the major DHI to streamflow

Overall, the spatial patterns of water withdrawal changes (Figure 7c) are similar to MAF changes induced by DHI change (ΔQ_h, Figure 5c) between the two sub-periods. Though water use partly infiltrates into land surface and eventually increases local runoff (see Figure 7d), water withdrawals should be the major DHI that contributes to decreases in streamflow in most river segments in China. For example, the significant decreases in MAF are supposed to be largely related to water withdrawals in the Northwest Rivers where streamflow is low and only one reservoir was included in the VARSOC simulations. The water withdrawal changes in Northwest Rivers are relatively small compared to other northern basins, but they still have significant implications because of the limited water resources. As mentioned above, water withdrawal for agricultural irrigation accounts for the largest proportion of human water use in China, most of which evaporates into the atmosphere finally through both crop and soil because of the low irrigation efficiencies (Zhu et al., 2013), which might be the main source depleting the streamflow and local water resources. Though the return flow might increase runoff over most river segments of China (Figure 7d), it seems to be only a small proportion of the water withdrawals and does not offset the decreases in streamflow. Unlike water withdrawals, the effects of reservoir regulation on annual streamflow are mixed in current GHMs as reservoir regulation generally reduces streamflow in flood (and growing) seasons while streamflow increases in dry seasons (Masaki et al., 2017).

4.4 Increasing DHI may impair the adaptive capacity of freshwater system

Though the effects of DHI change on streamflow are smaller compared to those of climate variability change in China (see section 4.2), the DHI-induced streamflow changes significantly increased particularly in the northern basins over the 1971-2010 period (Figure 3). The northern basins have relatively poor water endowments and have been identified as regions that are highly sensitive to climate change (Piao et al., 2010). The relatively high DHI further increase the pressure and threats to water management and adaptation to future climate change in these regions. For example, frequent zero flow was observed in some reaches of the Yellow River due to climate variability change and human water use in the 1990s (Tang et al., 2013).

Most northern regions suffered severe water scarcity during the past decades (Liu et al., 2017a), and the water resources have been increasingly insufficient for human water needs in many areas of northern basins (Liu and Xia, 2004). The unregulated pumping of non-renewable groundwater has resulted in significant depletion and far-reaching effects on both hydrological cycle and human society in these regions (Feng et al., 2013). The DHI change over time further enlarges associated streamflow changes in these basins (see Figure 4c and Figure S4S5). The situation could be worse if no adaptation is taken to act under future climate change (Piao et al., 2010; Liu et al., 2015). Thus, in view of the considerable DHI in these regions, there is an urgent need for a structural transformation of the economy towards reducing water use and a sustainable development.

4.5 Uncertainties in the quantitative assessment

The major uncertainty in this quantitative assessment usually originates from input forcings (Müller Schmied et al., 2014) and inter-model differences such as human impact parameterizations (Liu et al., 2017b). That is, the uncertainties in streamflow simulations would propagate to the assessment. For example, there are very few meteorological observations in the Northwest Rivers, possibly leading to considerable uncertainties in the meteorological forcings used to drive GHMs. Furthermore, the GHMs cannot fully reflect sectoral water withdrawals (Figure 2; also see Huang et al., 2018; also see Figure 2) because of lacking data on water abstractions for human use from surface and groundwater sources (Liu et al., 2017b). Meanwhile, the different water withdrawal requirement and withdrawal sources considered in GHMs (see Table 1) may result in inter-model uncertainty in the estimates of water withdrawals and perhaps enlarge the discrepancy in streamflow simulations. The multimodel ensemble medians seem to be in line with observations averaged across the stations in China, but large discrepancies are found in some basins (Figure S2). This indicates a large space for the GHMs to improve streamflow simulations in China. It should be noted that we have relocated some stations on the map to reconcile the catchment areas of the stations and the corresponding grid cells on the DDM30 river network. However, catchment areas still are inconsistent between some stations and their corresponding grid cells, especially for the stations not on the main stream. This may be partly responsible for the deviation between simulated and observed streamflow. More hydrological observations (from large catchment areas) are necessary to perform a comprehensive evaluation of streamflow simulations.

In addition to the uncertainties in multimodel simulations of streamflow, the quantitative assessment depends on the selection of comparison periods (see Table S7). To examine the possible effects of the selection of sub-periods, we perform similar assessments for different sub-periods, i.e., MAF changes of three decades of 1981-1990, 1991-2000, and 2001-2010 compared to the first decade (1971-1980). The assessments show similar patterns of MAF changes as in Figure 5, with larger relative changes in most northern basins (see Figure S4 S5 for the analysis at basin scale). Effects of climate variability change on streamflow vary over different sub-periods. In contrast, DHI change usually resulted in MAF decrease across all basins and its impact slightly increases over time (see Table S6 S7 for corresponding numbers), especially in the northern basins such as the Yellow River, the Northwest Rivers, the Liao River, and the Hai River. In the Yellow River, MAF changes induced by DHI change outweigh that induced by climate variability change in the 2001-2010 period. Human activities may be weaker in

China before the year 1971, and the DHI change could be larger if compared to earlier periods (e.g., Müller Schmied et al., 2016). This assessment suggests that the magnitudes of the impacts of both climate variability ~~change~~ and DHI change on streamflow are associated with specific sub-periods, however, DHI change decreased streamflow in almost all basins in the study period.

4.6 Comparison with previous studies

Both this study and previous ones (~~see~~ Table ~~S7~~S8) show that DHI (change) almost always contributes to decreases in streamflow in China, but the DHI contributions are much more significant in previous assessments compared to this one. Previous studies have shown that DHI contributed to decrease in streamflow by 20% to 80% across catchments in the Hai River, Yellow River and Huai River (see Table ~~S7~~S8, it should be noted that the proportions in the table were calculated as $100\times\Delta Q_h/\Delta Q_a$). In four cases the DHI contributions are larger than those of climate ~~change~~ impact and in most cases DHI contribute more than 40% in these studies (see Table ~~S7~~ S8 for the results from previous studies), while DHI contributions are mostly smaller than climate variability ~~change~~ in this assessment (Figure 6a). There are several reasons for the large differences between this assessment and previous ones which make their results not comparable directly, such as different methods and data, sub-periods, and study areas (see ~~Figure~~ Table ~~S7~~ S8 for details). Unlike this study, ~~T~~the previous assessments were usually performed in small catchments where experienced evident human activities and usually chose comparison periods by using statistical approaches (e.g., abrupt-changing point detection for a time series).

One major difference between previous studies (e.g., Li et al., 2007; Bao et al., 2012) and this study is that the former estimates DHI contribution by comparing simulations with observations while we compare two simulation experiments. The former may be subject to uncertainty in comparing the data from two systems (i.e., the model and the real world). In this study, the two simulation experiments favor the estimation of DHI contribution in a consistent manner that is largely free of uncertainty in the data from different systems. The multimodel simulations also allow profiling the uncertainties among models and input forcings, which is difficult for a single model assessment. However, the deficiency of this approach is that DHI is not real. Therefore, the assessment is inevitably influenced by the extent to which the models can reproduce the real DHI. ~~In contrast with previous studies, the multimodel simulations facilitate the attribution of DHI (change) on streamflow in a consistent manner that is largely free of the uncertainty of data from different systems (i.e., modeling and observation). They also allow profiling the uncertainties among models and input forcings, which is difficult for a single model assessment.~~ Considering the complexity of DHI on streamflow and the ability of current hydrological models in reproducing historical hydrological changes, multimodel simulations and different attribution approaches are well worth obtaining more robust assessments (Liu et al., 2017b; Yuan et al., 2018).

5 Conclusions

A quantitative assessment of the contributions of DHI (direct human impact) and climate ~~change~~ impact on streamflow changes is performed in the ten major river basins in China during the 1971-2010 period. The ISIMIP2a multimodel simulations are evaluated against hydrological observations in China and are used for the assessment. The results show that DHI caused decreases of one-fifth to one-third of the long-term MAF in the sub-periods of 1971-1990 and 1991-2010 in most northern basins. MAF changes between the two sub-periods are small in southern basins but are relatively large in northern basins where MAF decrease by 10% or more. It is found that DHI change between the two sub-periods resulted in MAF decreases in 70% of the river segments. However, total MAF changes are dominated by climate variability ~~change~~ in 88% of the river segments of China. The respective contributions of climate and DHI changes to streamflow changes are more pronounced in northern basins. The relative contribution of DHI change shows significant regional difference with relatively larger values in northern basins (-3% to -8% of MAF) and smaller ones in southern basins (-0.7% to -0.07%). The contribution of climate variability ~~change~~ to streamflow changes varies between basins, ranging from -9% to 18% of MAF in northern basins and from -1.6% to 1.3% in southern basins. The same analyses for different sub-periods, i.e., the 1980s, 1990s, and 2000s compared with the 1970s, show similar spatial patterns of the contribution of DHI change. It indicates that human intervention is high in northern basins with an increasing trend over time, which likely impairs the adaptive capacity of freshwater system under future climate change. This assessment also shows that water withdrawals are the major factor that directly affects streamflow in China. It should be noted that this assessment is subject to uncertainties arising from the uncertainties in multimodel simulations and the choice of study periods. Nevertheless, it can serve as a reference, in a socio-hydrological perspective, for the attribution of changes in streamflow at large scales under a changing environment. We highlight the importance of reducing DHI on streamflow for a sustainable development in northern basins of China and expect the assessment to favor China’s strategy on adaptation to future climate change.

Data availability. All model data used in this study can be accessed by the public following the instructions on the website of the Inter-Sectoral Impact Model Intercomparison Project (www.isimip.org).

Author contribution. XL, QT, WL, HY designed the research; XL, MF, YM, HMS, SO, YP, YS, YW prepared the model data; XL performed the analyses and wrote the draft, and all authors wrote the manuscript.

Competing interests. The authors declare that they have no conflict of interest.

Acknowledgments

We thank the Inter-Sectoral Impact Model Intercomparison Project coordinating team for providing the simulated data. This research is supported by the National Natural Science Foundation of China (41730645, 41425002, 41790424, and 41877164), the Key Research Program of the Chinese Academy of Sciences (KGFZD-135-17-009-3, ZDRW-ZS-2017-4), and the

International Partnership Program of Chinese Academy of Sciences (131A11KYSB20170113). W.L. acknowledges the support received from the Early Postdoctoral Mobility Fellowship awarded by the Swiss National Science Foundation (P2EZP2_175096). Y.P. acknowledges the support from the Asian Studies Center at Michigan State University.

References

Biemans, H., Haddeland, I., Kabat, P., Ludwig, F., Hutjes, R. W. A., Heinke, J., von Bloh, W., and Gerten, D.: Impact of reservoirs on river discharge and irrigation water supply during the 20th century, Water Resour. Res., 47, W03509, 10.1029/2009WR008929, 2011.

Bondeau, A., Smith, P. C., Zaehle, S., Schaphoff, S., Lucht, W., Cramer, W., Gerten, D., Lotze-Campen, H., Müller, C., Reichstein, M., and Smith, B.: Modelling the role of agriculture for the 20th century global terrestrial carbon balance, Global Change Biol., 13, 679-706, 10.1111/j.1365-2486.2006.01305.x, 2007.

Bosmans, J. H. C., van Beek, L. P. H., Sutanudjaja, E. H., and Bierkens, M. F. P.: Hydrological impacts of global land cover change and human water use, Hydrol. Earth Syst. Sci., 21, 5603-5626, 10.5194/hess-21-5603-2017, 2017.

Chang, J., H. Zhang, Y. Wang, and Y. Zhu (2016), Assessing the impact of climate variability and human activities on streamflow variation, Hydrol. Earth Syst. Sci., 20(4), 1547-1560, doi: 10.5194/hess-20-1547-2016.

Döll, P., and Lehner, B.: Validation of a new global 30-min drainage direction map, J. Hydrol., 258, 214-231, 10.1016/S0022-1694(01)00565-0, 2002.

Döll, P., Douville, H., Güntner, A., Müller Schmied, H., and Wada, Y.: Modelling Freshwater Resources at the Global Scale: Challenges and Prospects, Surv. Geophys., 37, 195-221, 10.1007/s10712-015-9343-1, 2016.

Döll, P., Fiedler, K., and Zhang, J.: Global-scale analysis of river flow alterations due to water withdrawals and reservoirs, Hydrol. Earth Syst. Sci., 13, 2413-2432, 10.5194/hess-13-2413-2009, 2009.

Fader, M., Rost, S., Müller, C., Bondeau, A., and Gerten, D.: Virtual water content of temperate cereals and maize: Present and potential future patterns, J. Hydrol., 384, 218-231, 10.1016/j.jhydrol.2009.12.011, 2010.

Feng, W., Zhong, M., Lemoine, J.-M., Biancale, R., Hsu, H.-T., and Xia, J.: Evaluation of groundwater depletion in North China using the Gravity Recovery and Climate Experiment (GRACE) data and ground-based measurements, Water Resour. Res., 49, 2110-2118, 10.1002/wrcr.20192, 2013.

Ficklin, D. L., Abatzoglou, J. T., Robeson, S. M., Null, S. E., and Knouft, J. H.: Natural and managed watersheds show similar responses to recent climate change, Proc. Nat. Acad. Sci., 115, 8553-8557, 10.1073/pnas.1801026115, 2018.

Flörke, M., Kynast, E., Bärlund, I., Eisner, S., Wimmer, F., and Alcamo, J.: Domestic and industrial water uses of the past 60 years as a mirror of socio-economic development: A global simulation study, Global Environ. Change, 23, 144-156, 10.1016/j.gloenvcha.2012.10.018, 2013.

Gosling, S., Müller Schmied, H., Betts, R., Chang, J., Ciais, P., Dankers, R., Döll, P., Eisner, S., Flörke, M., Gerten, D., Grillakis, M., Hanasaki, N., Hagemann, S., Huang, M., Huang, Z., Jerez, S., Kim, H., Koutroulis, A., Leng, G., Liu, X., Masaki, Y., Montavez, P., Morfopoulos, C., Oki, T., Papadimitriou, L., Pokhrel, Y., Portmann, F. T., Orth, R., Ostberg, S., Satoh, Y., Seneviratne, S., Sommer, P., Stacke, T., Tang, Q., Tsanis, I., Wada, Y., Zhou, T., Büchner, M., Schewe, J., and Zhao, F.: ISIMIP2a simulation data from water (global) sector, GFZ Data Services, 2017.

Haddeland, I., Heinke, J., Biemans, H., Eisner, S., Flörke, M., Hanasaki, N., Konzmann, M., Ludwig, F., Masaki, Y., Schewe, J., Stacke, T., Tessler, Z. D., Wada, Y., and Wisser, D.: Global water resources affected by human interventions and climate change, Proc. Nat. Acad. Sci., 111, 3251-3256, 10.1073/pnas.1222475110, 2014.

Hanasaki, N., Kanae, S., Oki, T., Masuda, K., Motoya, K., Shirakawa, N., Shen, Y., and Tanaka, K.: An integrated model for the assessment of global water resources – Part 1: Model description and input meteorological forcing, Hydrol. Earth Syst. Sci., 12, 1007-1025, 10.5194/hess-12-1007-2008, 2008a.

Hanasaki, N., Kanae, S., Oki, T., Masuda, K., Motoya, K., Shirakawa, N., Shen, Y., and Tanaka, K.: An integrated model for the assessment of global water resources – Part 2: Applications and assessments, Hydrol. Earth Syst. Sci., 12, 1027-1037, 10.5194/hess-12-1027-2008, 2008b.

Huang, Z., Hejazi, M., Li, X., Tang, Q., Vernon, C., Leng, G., Liu, Y., Döll, P., Eisner, S., Gerten, D., Hanasaki, N., and Wada, Y.: Reconstruction of global gridded monthly sectoral water withdrawals for 1971–2010 and analysis of their spatiotemporal patterns, Hydrol. Earth Syst. Sci., 22, 2117-2133, 10.5194/hess-22-2117-2018, 2018.

Ian, M. F., and Reed, M. M.: Human impacts on terrestrial hydrology: climate change versus pumping and irrigation, Environ. Res. Lett., 7, 044022, 10.1088/1748-9326/7/4/044022, 2012.

Jaramillo, F., and Destouni, G.: Local flow regulation and irrigation raise global human water consumption and footprint, Science, 350, 1248-1251, 10.1126/science.aad1010, 2015.

Lehner, B., Liermann, C. R., Revenga, C., Vörösmarty, C., Fekete, B., Crouzet, P., Döll, P., Endejan, M., Frenken, K., Magome, J., Nilsson, C., Robertson, J. C., Rödel, R., Sindorf, N., and Wisser, D.: High-resolution mapping of the world's reservoirs and dams for sustainable river-flow management, Frontiers in Ecology and the Environment, 9, 494-502, 10.1890/100125, 2011.

Li, L., Zhang, L., Wang, H., Wang, J., Yang, J., Jiang, D., Li, J., and Qin, D.: Assessing the impact of climate variability and human activities on streamflow from the Wuding River basin in China, Hydrol. Processes, 21, 3485-3491, doi:10.1002/hyp.6485, 2007.

Liu, C., and Xia, J.: Water problems and hydrological research in the Yellow River and the Huai and Hai River basins of China, Hydrol. Processes, 18, 2197-2210, 2004.

Liu, J., Yang, H., Gosling, S. N., Kummu, M., Flörke, M., Pfister, S., Hanasaki, N., Wada, Y., Zhang, X., Zheng, C., Alcamo, J., and Oki, T.: Water scarcity assessments in the past, present, and future, Earth's Future, 5, 545-559, 10.1002/2016EF000518, 2017a.

Liu, L., and Du, J.: Documented changes in annual runoff and attribution since the 1950s within selected rivers in China, Adv. Clim. Change Res., 8, 37-47, 10.1016/j.accre.2017.03.005, 2017.

Liu, X., Liu, C., Luo, Y., Zhang, M., and Xia, J.: Dramatic decrease in streamflow from the headwater source in the central route of China's water diversion project: Climatic variation or human influence?, J Geophys Res: Atmos, 117, doi:10.1029/2011JD016879, 2012.

Liu, X., Tang, Q., Cui, H., Mengfei, M., Gerten, D., Gosling, S., Masaki, Y., Satoh, Y., and Wada, Y.: Multimodel uncertainty changes in simulated river flows induced by human impact parameterizations, Environ. Res. Lett., 12, 025009, 10.1088/1748-9326/aa5a3a, 2017b.

Liu, X., Tang, Q., Zhang, X., and Leng, G.: Modeling the role of vegetation in hydrological responses to climate change, in: Terrestrial water cycle and climate change: Natural and human-induced impacts, edited by: Tang, Q., and Oki, T., John Wiley & Sons, Inc., Hoboken, New Jersey, 193-208, 2016.

Liu, X., Zhang, X., Tang, Q., and Zhang, X.: Effects of surface wind speed decline on modeled hydrological conditions in China, Hydrol. Earth Syst. Sci., 18, 2803-2813, 10.5194/hess-18-2803-2014, 2014.

Liu, Y., Pan, Z., Zhuang, Q., Miralles, D. G., Teuling, A. J., Zhang, T., An, P., Dong, Z., Zhang, J., He, D., Wang, L., Pan, X., Bai, W., and Niyogi, D.: Agriculture intensifies soil moisture decline in Northern China, Sci. Rep., 5, 11261, 10.1038/srep11261, 2015.

Masaki, Y., Hanasaki, N., Biemans, H., Müller Schmied, H., Tang, Q., Wada, Y., Gosling, S. N., Takahashi, K., and Hijioka, Y.: Intercomparison of global river discharge simulations focusing on dam operation—multiple models analysis in two case-study river basins, Missouri–Mississippi and Green–Colorado, Environ. Res. Lett., 12, 055002, 2017.

Müller Schmied, H., Adam, L., Eisner, S., Fink, G., Flörke, M., Kim, H., Oki, T., Portmann, F. T., Reinecke, R., Riedel, C., Song, Q., Zhang, J., and Döll, P.: Variations of global and continental water balance components as impacted by climate forcing uncertainty and human water use, Hydrol. Earth Syst. Sci., 20, 2877-2898, 10.5194/hess-20-2877-2016, 2016.

Müller Schmied, H., Eisner, S., Franz, D., Wattenbach, M., Portmann, F. T., Flörke, M., and Döll, P.: Sensitivity of simulated global-scale freshwater fluxes and storages to input data, hydrological model structure, human water use and calibration, Hydrol. Earth Syst. Sci., 18, 3511-3538, 10.5194/hess-18-3511-2014, 2014.

Oki, T., and S. Kanae (2006), Global hydrological cycles and world water resources, Science, 313(5790), 1068-1072, doi: 10.1126/science.1128845.

Patterson, L. A., Lutz, B., and Doyle, M. W.: Climate and direct human contributions to changes in mean annual streamflow in the South Atlantic, USA, Water Resour. Res., 49, 7278-7291, doi:10.1002/2013WR014618, 2013.

Piao, S., Ciais, P., Huang, Y., Shen, Z., Peng, S., Li, J., Zhou, L., Liu, H., Ma, Y., Ding, Y., Friedlingstein, P., Liu, C., Tan, K., Yu, Y., Zhang, T., and Fang, J.: The impacts of climate change on water resources and agriculture in China, Nature, 467, 43, 10.1038/nature09364, 2010.

Pokhrel, Y. N., Hanasaki, N., Wada, Y., and Kim, H.: Recent progresses in incorporating human land–water management into global land surface models toward their integration into Earth system models, WIREs: Water, 3, 548-574, 10.1002/wat2.1150, 2016.

Pokhrel, Y. N., Koirala, S., Yeh, P. J. F., Hanasaki, N., Longuevergne, L., Kanae, S., and Oki, T.: Incorporation of groundwater pumping in a global Land Surface Model with the representation of human impacts, Water Resour. Res., 51, 78-96, 10.1002/2014WR015602, 2015.

Portmann, F. T., Siebert, S., and Döll, P.: MIRCA2000—Global monthly irrigated and rainfed crop areas around the year 2000: A new high-resolution data set for agricultural and hydrological modeling, Global Biogeochem. Cycles, 24, GB1011, 10.1029/2008GB003435, 2010.

Rost, S., Gerten, D., Bondeau, A., Lucht, W., Rohwer, J., and Schaphoff, S.: Agricultural green and blue water consumption and its influence on the global water system, Water Resour. Res., 44, W09405, 10.1029/2007WR006331, 2008.

Schaphoff, S., Heyder, U., Ostberg, S., Gerten, D., Heinke, J., and Lucht, W.: Contribution of permafrost soils to the global carbon budget, Environ. Res. Lett., 8, 014026, 2013.

Sheffield, J., Goteti, G., and Wood, E. F.: Development of a 50-year high-resolution global dataset of meteorological forcings for land surface modeling, J. Climate, 19, 3088-3111, 10.1175/jcli3790.1, 2006.

Takata, K., Emori, S., and Watanabe, T.: Development of the minimal advanced treatments of surface interaction and runoff, Global Planet. Change, 38, 209-222, 10.1016/S0921-8181(03)00030-4, 2003.

Tan, X., and Gan, T. Y.: Contribution of human and climate change impacts to changes in streamflow of Canada, Sci. Rep., 5, 17767, 10.1038/srep17767, 2015.

Tang, Q., and Oki, T.: Terrestrial Water Cycle and Climate Change: Natural and Human-Induced Impacts, AGU Geophysical Monograph Series, John Wiley & Sons, Hoboken, New Jersey, 246 pp., 2016.

Tang, Q., Oki, T., Kanae, S., and Hu, H.: The influence of precipitation variability and partial irrigation within grid cells on a hydrological simulation, J. Hydrometeor, 8, 499-512, 10.1175/jhm589.1, 2007.

Tang, Q., Oki, T., Kanae, S., and Hu, H.: Hydrological Cycles Change in the Yellow River Basin during the Last Half of the Twentieth Century, J. Climate, 21, 1790-1806, 10.1175/2007JCLI1854.1, 2008.

Tang, Y., Tang, Q., Tian, F., Zhang, Z., and Liu, G.: Responses of natural runoff to recent climatic variations in the Yellow River basin, China, Hydrol. Earth Syst. Sci., 17, 4471-4480, 10.5194/hess-17-4471-2013, 2013.

Veldkamp, T. I. E., Wada, Y., Aerts, J. C. J. H., Doll, P., Gosling, S. N., Liu, J., Masaki, Y., Oki, T., Ostberg, S., Pokhrel, Y., Satoh, Y., Kim, H., and Ward, P. J.: Water scarcity hotspots travel downstream due to human interventions in the 20th and 21st century, Nat. Commun., 8, 15697, 10.1038/ncomms15697, 2017.

Veldkamp, T. I. E., Zhao, F., Ward, P. J., Moel, H. d., Aerts, J. C. J. H., Schmied, H. M., Portmann, F. T., Masaki, Y., Pokhrel, Y., Liu, X., Satoh, Y., Gerten, D., Gosling, S. N., Zaherpour, J., and Wada, Y.: Human impact parameterizations in global hydrological models improve estimates of monthly discharges and hydrological extremes: a multi-model validation study, Environ. Res. Lett., 13, 055008, 10.1088/1748-9326/aab96f, 2018.

Wada, Y., and Heinrich, L.: Assessment of transboundary aquifers of the world—vulnerability arising from human water use, Environ. Res. Lett., 8, 024003, 10.1088/1748-9326/8/2/024003, 2013.

Wada, Y., Bierkens, M. F. P., de Roo, A., Dirmeyer, P. A., Famiglietti, J. S., Hanasaki, N., Konar, M., Liu, J., Müller Schmied, H., Oki, T., Pokhrel, Y., Sivapalan, M., Troy, T. J., van Dijk, A. I. J. M., van Emmerik, T., Van Huijgevoort, M. H. J., Van Lanen, H. A. J., Vörösmarty, C. J., Wanders, N., and Wheater, H.: Human–water interface in hydrological modelling: current status and future directions, Hydrol. Earth Syst. Sci., 21, 4169-4193, 10.5194/hess-21-4169-2017, 2017.

Wada, Y., Wisser, D., and Bierkens, M. F. P.: Global modeling of withdrawal, allocation and consumptive use of surface water and groundwater resources, Earth Syst. Dynam., 5, 15-40, 10.5194/esd-5-15-2014, 2014.

Wada, Y., Bierkens, M. F. P., de Roo, A., Dirmeyer, P. A., Famiglietti, J. S., Hanasaki, N., Konar, M., Liu, J., Müller Schmied, H., Oki, T., Pokhrel, Y., Sivapalan, M., Troy, T. J., van Dijk, A. I. J. M., van Emmerik, T., Van Huijgevoort, M. H. J., Van Lanen, H. A. J., Vörösmarty, C. J., Wanders, N., and Wheater, H.: Human–water interface in hydrological modelling: current status and future directions, Hydrol. Earth Syst. Sci., 21, 4169-4193, 10.5194/hess-21-4169-2017, 2017.

Wada, Y., van Beek, L. P. H., Wanders, N., and Bierkens, M. F. P.: Human water consumption intensifies hydrological drought worldwide, Environ. Res. Lett., 8, 034036, 2013.

Wang, G., Xia, J., and Chen, J.: Quantification of effects of climate variations and human activities on runoff by a monthly water balance model: A case study of the Chaobai River basin in northern China, Water Resour. Res., 45, doi:10.1029/2007WR006768, 2009.

Wang, J., Sheng, Y., and Wada, Y.: Little impact of the Three Gorges Dam on recent decadal lake decline across China's Yangtze Plain, Water Resour. Res., 53, 3854-3877, doi:10.1002/2016WR019817, 2017.

Wang, J., Hong, Y., Gourley, J., Adhikari, P., Li, L., and Su, F.: Quantitative assessment of climate change and human impacts on long-term hydrologic response: a case study in a sub-basin of the Yellow River, China, Int. J. Climatol., 30, 2130-2137, doi:10.1002/joc.2023, 2010.

Wang, J., Sheng, Y., Gleason, C. J., and Wada, Y.: Downstream Yangtze River levels impacted by Three Gorges Dam, Environ. Res. Lett., 8, 044012, 2013a.

Wang, W., Shao, Q., Yang, T., Peng, S., Xing, W., Sun, F., and Luo, Y.: Quantitative assessment of the impact of climate variability and human activities on runoff changes: a case study in four catchments of the Haihe River basin, China, Hydrol. Processes, 27, 1158-1174, doi:10.1002/hyp.9299, 2013b.

Weedon, G. P., Balsamo, G., Bellouin, N., Gomes, S., Best, M. J., and Viterbo, P.: The WFDEI meteorological forcing data set: WATCH Forcing Data methodology applied to ERA-Interim reanalysis data, Water Resour. Res., 50, 7505-7514, 10.1002/2014WR015638, 2014.

Weedon, G. P., Gomes, S., Viterbo, P., Shuttleworth, W. J., Blyth, E., Österle, H., Adam, J. C., Bellouin, N., Boucher, O., and Best, M.: Creation of the WATCH Forcing Data and its use to assess global and regional reference crop evaporation over land during the twentieth century, J. Hydrometeor, 12, 823-848, 10.1175/2011jhm1369.1, 2011.

Yang, X., and Lu, X.: Drastic change in China's lakes and reservoirs over the past decades, Sci. Rep., 4, 6041, 10.1038/srep06041, 2014.

Ye, X., Zhang, Q., Liu, J., Li, X., and Xu, C.-y.: Distinguishing the relative impacts of climate change and human activities on variation of streamflow in the Poyang Lake catchment, China, J. Hydrol., 494, 83-95, 10.1016/j.jhydrol.2013.04.036, 2013.

Yin, Y., Tang, Q., Liu, X., and Zhang, X.: Water scarcity under various socio-economic pathways and its potential effects on food production in the Yellow River basin, Hydrol. Earth Syst. Sci., 21, 791-804, 10.5194/hess-21-791-2017, 2017.

Yuan, X., Jiao, Y., Yang, D., and Lei, H.: Reconciling the attribution of changes in streamflow extremes from a hydroclimate perspective, Water Resour. Res., doi:10.1029/2018WR022714, 2018.

Zaherpour, J., Gosling, S. N., Mount, N., Schmied, H. M., Veldkamp, T. I. E., Dankers, R., Eisner, S., Gerten, D., Gudmundsson, L., Haddeland, I., Hanasaki, N., Kim, H., Leng, G., Liu, J., Masaki, Y., Oki, T., Pokhrel, Y., Satoh, Y., Schewe, J., and Wada, Y.: Worldwide evaluation of mean and extreme runoff from six global-scale hydrological models that account for human impacts, Environ. Res. Lett., 13, 065015, 10.1088/1748-9326/aac547, 2018.

Zhan, C., S. Jiang, F. Sun, Y. Jia, C. Niu, and W. Yue (2014), Quantitative contribution of climate change and human activities to runoff changes in the Wei River basin, China, Hydrol. Earth Syst. Sci., 18(8), 3069-3077, doi: 10.5194/hess-18-3069-2014.

Zhang, C., Tang, Q., and Chen, D.: Recent changes in the moisture source of precipitation over the Tibetan Plateau, J. Climate, 30, 1807-1819, 10.1175/jcli-d-15-0842.1, 2017.

Zhang, L., Dawes, W. R., and Walker, G. R.: Response of mean annual evapotranspiration to vegetation changes at catchment scale, Water Resour. Res., 37, 701-708, Doi 10.1029/2000wr900325, 2001.

Zhou, T., Nijssen, B., Gao, H., and Lettenmaier, D. P.: The contribution of reservoirs to global land surface water storage variations, J. Hydrometeor, 17, 309-325, 10.1175/JHM-D-15-0002.1, 2015.

Zhu, X., Li, Y., Li, M., Pan, Y., and Shi, P.: Agricultural irrigation in China, J. Soil Water Conserv., 68, 147A-154A, 10.2489/jswc.68.6.147A, 2013.

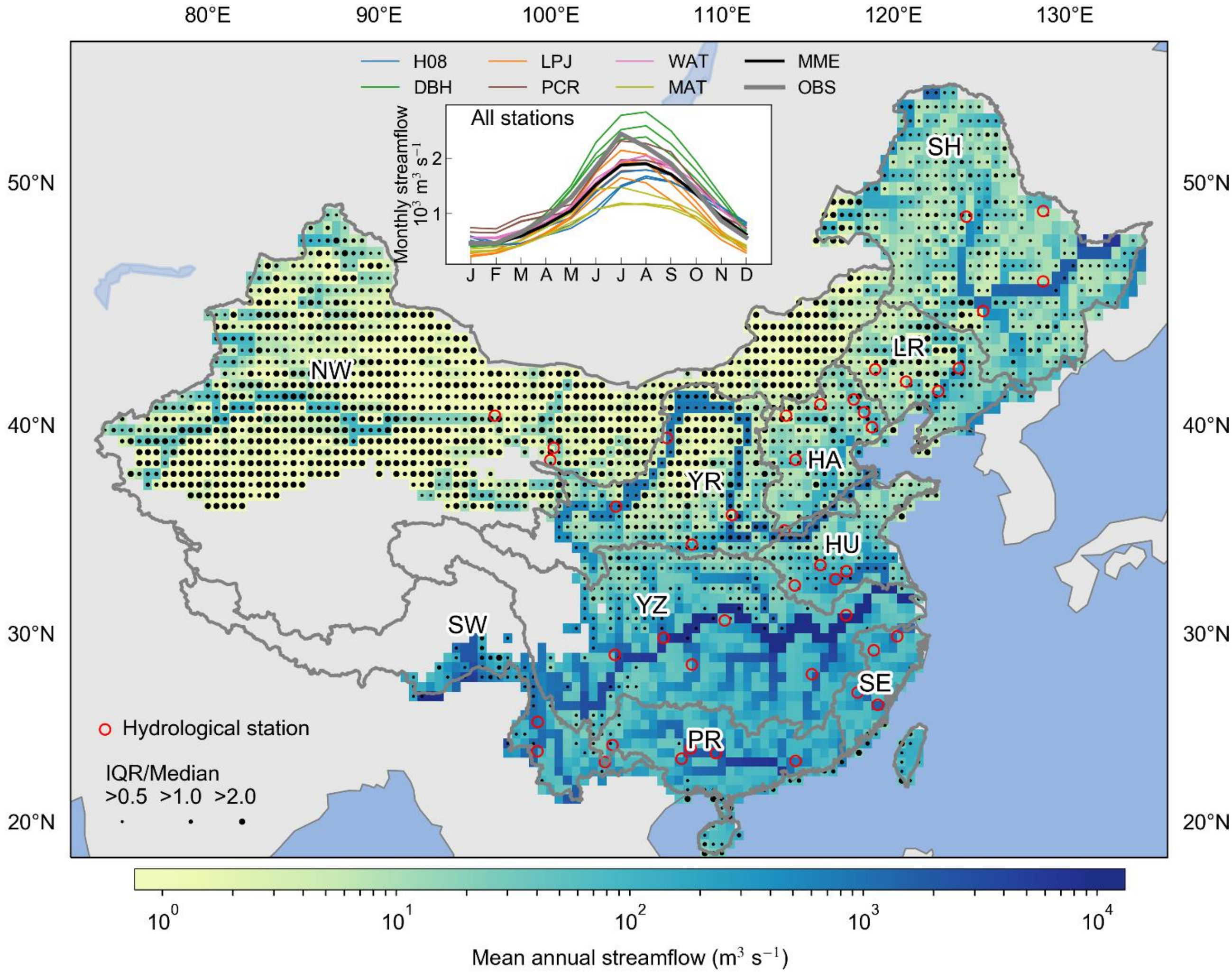

Figure 1. Multimodel medians of mean annual streamflow (MAF) in China from the VARSOC experiment. MAF medians are computed across 18 GHM-GMF combinations over the 1971-2000 period. The ensemble spread is represented by the ratio of interquartile range (IQR, 75th percentile minus 25th percentile) to the ensemble median of MAF (Median). The hydrological stations used in this study are identified by red circles. The inner plot shows the comparison of the simulated seasonal streamflow (each GHM has three lines for the three GMFs) from the VARSOC experiment against the observations averaged for all the hydrological stations shown on the map over the period 1971-2000. H08: H08, DBH: DBH, LPJ: LPJmL, PCR: PCR-GLOBWB, WAT: WaterGAP2, MAT: MATSIRO, MME: multimodel ensemble median, OBS: observation. The Tibetan Plateau region is masked by removing the grid cells with an altitude higher than 4000 meters, the same hereafter. The ten major basins in China are labeled and are indicated with grey lines. The southern basins include Yangtze River (YZ), Southwest Rivers (SW), Southeast Rivers (SE), and Pearl River (PR), the northern basins include Songhua River (SH), Liao River (LR), Northwest Rivers (NW), Hai River (HA), Yellow River (YR), and Huai River (HU).

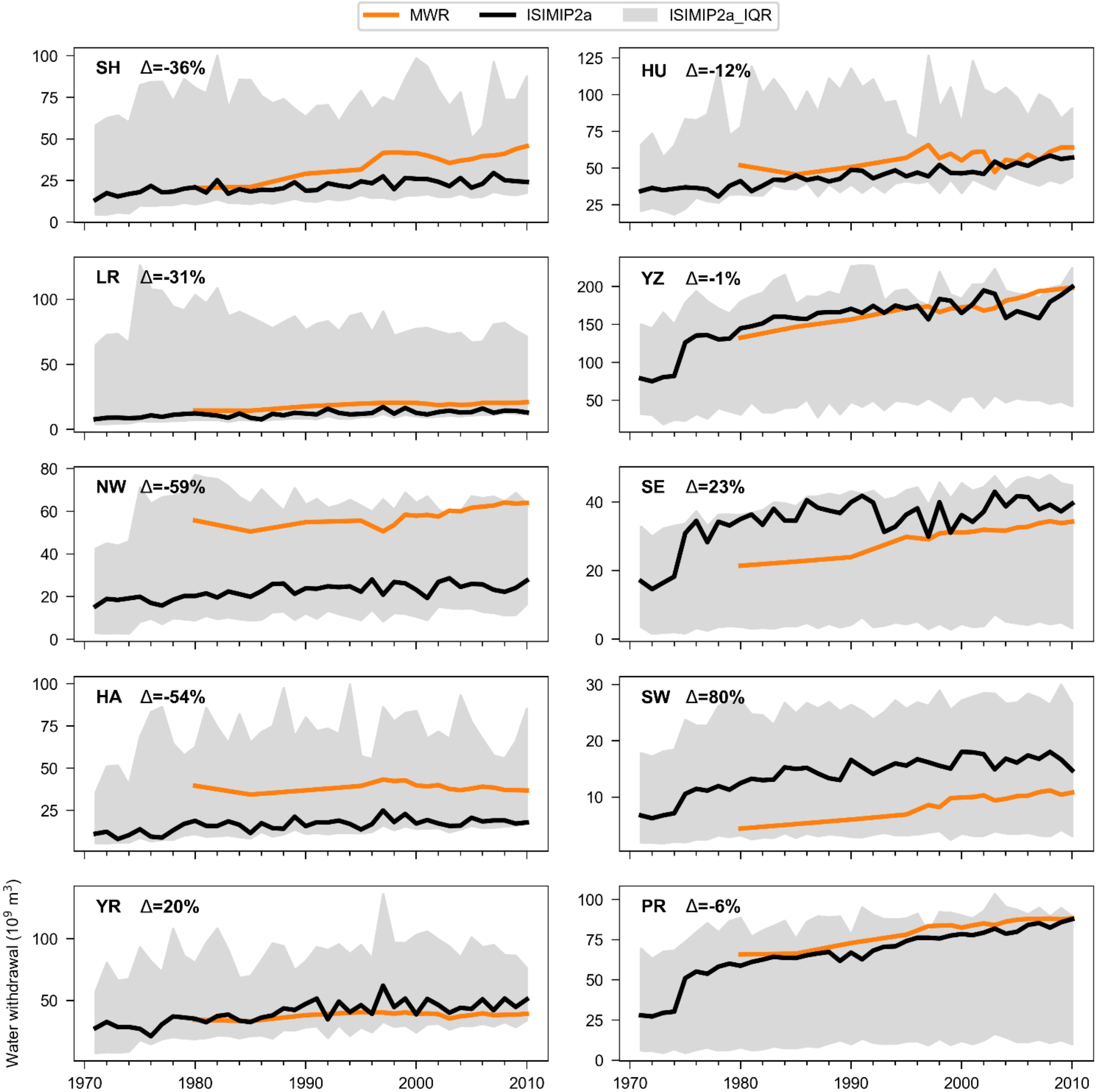

Figure 2. Reported and simulated water withdrawals in the 10 basins of China. ISIMIP2a indicates the simulated water withdrawals from the ISIMIP2a VARSOC experiment (see Table S1 for details) during 1971-2010; MWR indicates the water withdrawals reported by the Ministry of Water Resources (MWR) of China for the years of 1980, 1985, 1990, 1995, and 1997-2010. Δ indicates the difference between simulations and reported data. Shaded areas denote the IQR of ISIMIP2a simulations. The basin names labeled in each panel are corresponding to the basins in Figure 1.

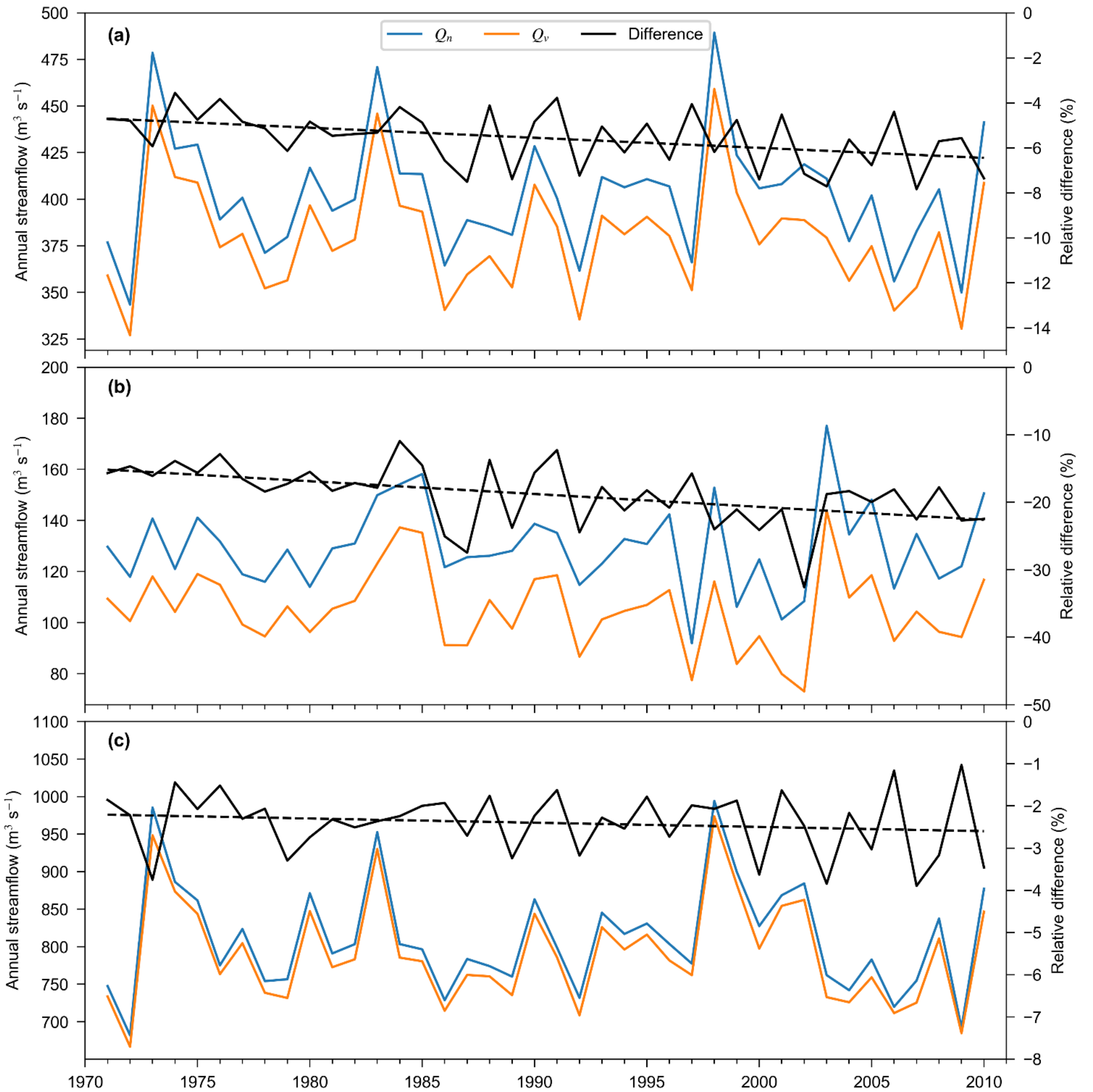

Figure 3. Spatially-averaged annual streamflows (m^3 s^{-1}) from NOSOC and VARSOC experiments and their differences (%) during the 1971-2010 period. (a) Average of ensemble medians of annual streamflow from NOSOC (Q_n) and VARSOC (Q_v) for China, (b) for the northern basins, and (c) for the southern basins. The northern and southern basins are described in Figure 1. The dashed lines denote the linear trend of the relative differences.

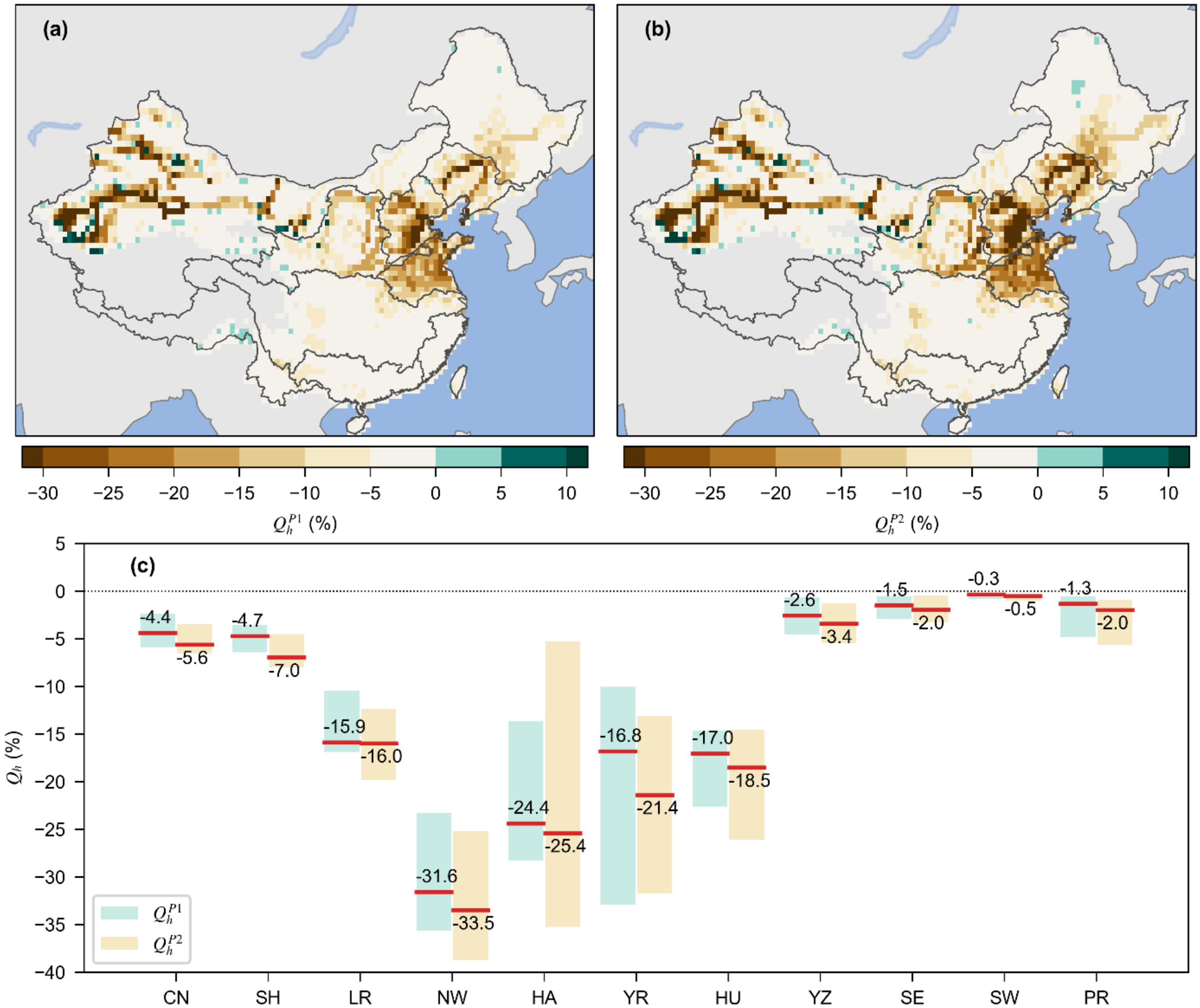

Figure 4. Long-term MAF altered by DHI. Ensemble medians of long-term MAF altered by DHI in (a) the sub-period 1971-1990 (Q_h^{P1}) and (b) the sub-period 1991-2010 (Q_h^{P2}), and (c) ensemble medians and ranges of averaged long-term MAF altered by DHI for each basin and China (denoted by CN). In plot (c), the range indicates the 25th and 75th values, and the numbers indicate the median values from all ensemble members.

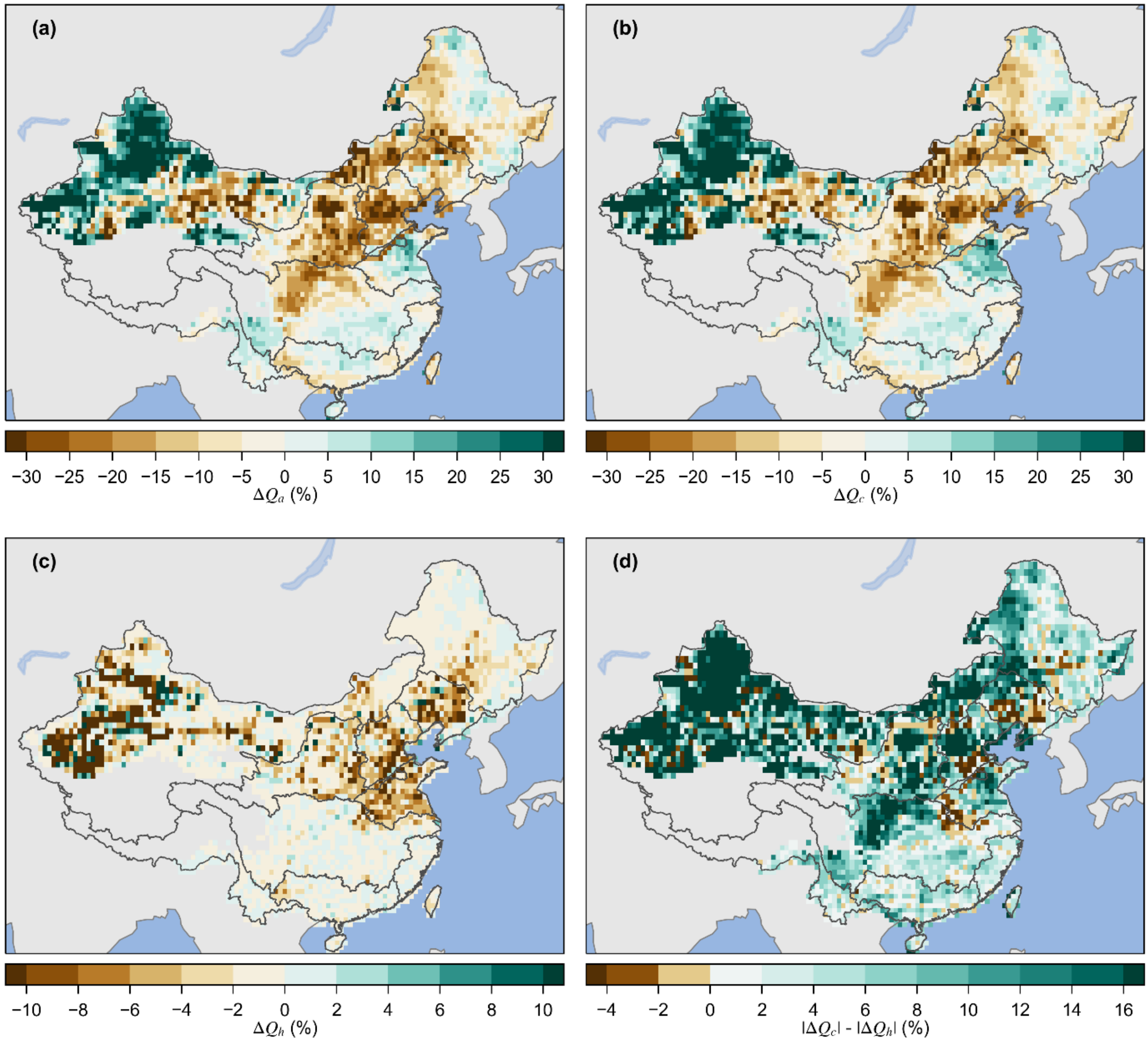

Figure 5. Relative changes (%) in long-term MAF over China between the two sub-periods (1971-1990 and 1991-2010). (a): Total MAF changes (ΔQ_a); (b): MAF changes induced by climate change (ΔQ_c); (c): MAF changes induced by DHI changes (ΔQ_h); (d): the difference between the magnitudes of ΔQ_c and ΔQ_h.

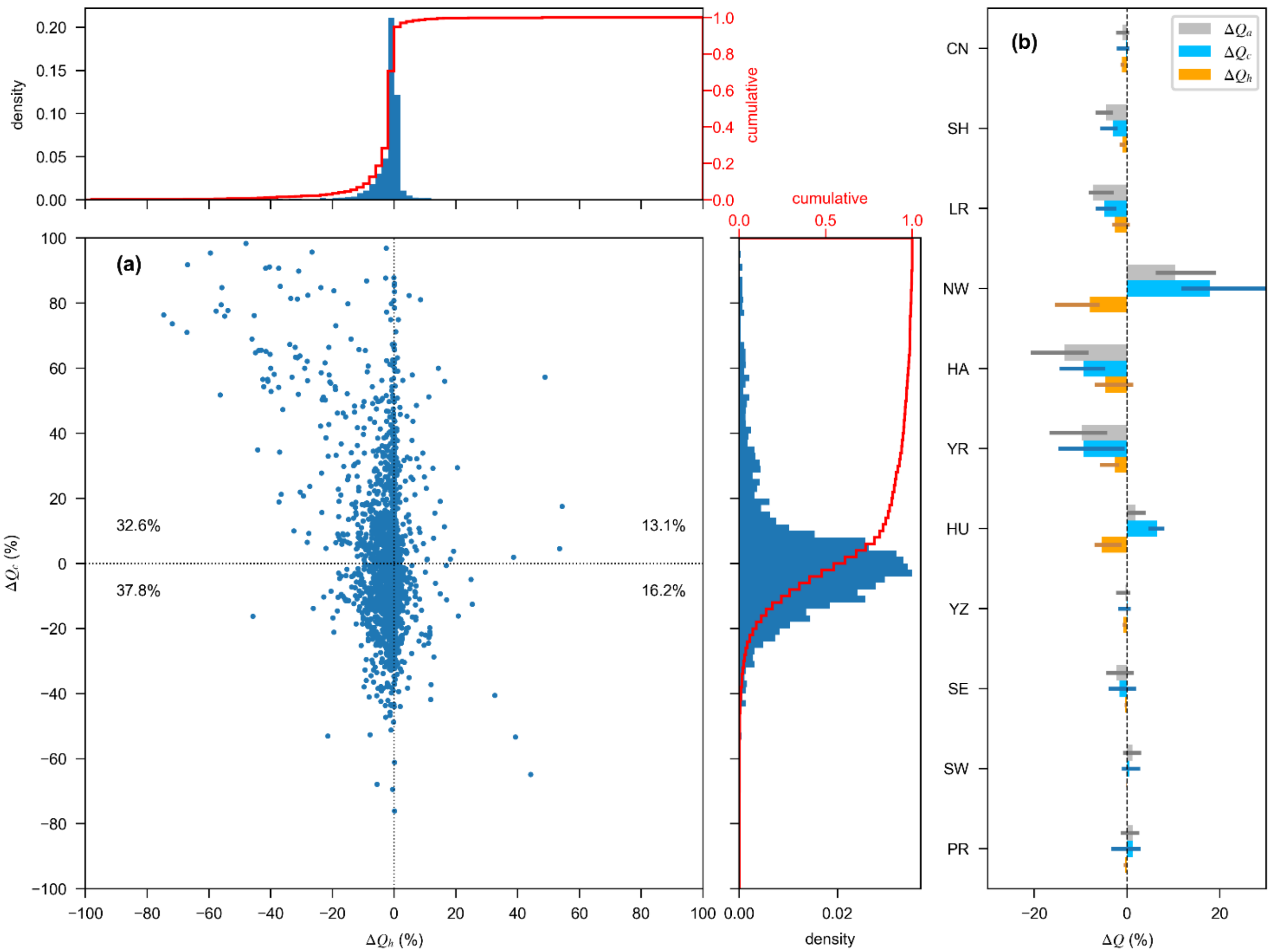

Figure 6. Relative MAF changes for river segments and basins. (a): ensemble medians of MAF changes induced by climate change (ΔQ_c) versus those induced by DHI change (ΔQ_h) for river segments of China; data points in (a) denote the values for individual river segments; the right histogram and the top histogram show the distributions of ΔQ_c and ΔQ_h, respectively; the numbers are the proportions of data points in each quadrant. (b): spatially aggregated ensemble medians of total MAF changes (ΔQ_a), MAF changes induced by climate change (ΔQ_c), and MAF changes induced by DHI change (ΔQ_h) for individual basins and China; the error bars indicate the IQR in each basin.

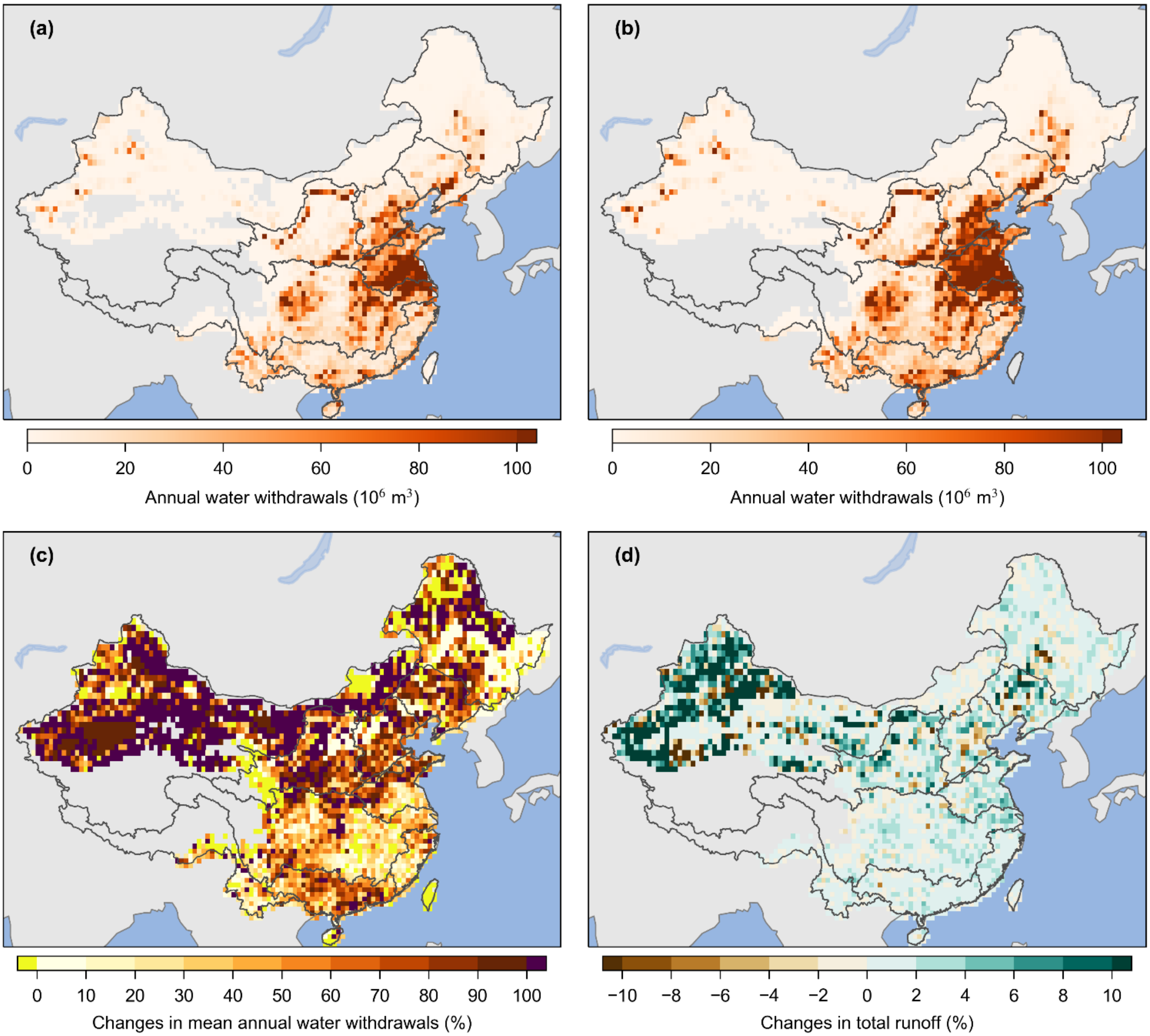

Figure 7. Changes in water withdrawals and total runoff between the two sub-periods. (a): ensemble medians of mean annual water withdrawals over the1971-1990 period; (b): ensemble medians of mean annual water withdrawals over 1991-2010 period; (c) ensemble medians of the changes in mean annual water withdrawals; (d): ensemble medians of the changes in mean annual total runoff.

Supplementary information

Multimodel assessments of human and climate impacts on mean annual streamflow in China

Xingcai Liu[1,2], Wenfeng Liu[2,3], Hong Yang[2,4], Qiuhong Tang[1,5], Martina Flörke[6], Yoshimitsu Masaki[7], Hannes Müller Schmied[8,9], Sebastian Ostberg[10], Yadu Pokhrel[11], Yusuke Satoh[12,13], Yoshihide Wada[12]

[1]Key Laboratory of Water Cycle and Related Land Surface Processes, Institute of Geographic Sciences and Natural Resources Research, Chinese Academy of Sciences, A11, Datun Road, Chaoyang District, Beijing, China

[2]Eawag, Swiss Federal Institute of Aquatic Science and Technology, Ueberlandstrasse 133, CH-8600 Duebendorf, Switzerland

[3]Laboratoire des Sciences du Climat et de l'Environnement, LSCE/IPSL, CEA-CNRS-UVSQ, Université Paris-Saclay, F-91191 Gif-sur-Yvette, France

[4]Department of Environmental Sciences, MGU, University of Basel, Petersplatz 1, CH-4003 Basel, Switzerland

[5]College of Resources and Environment, University of Chinese Academy of Sciences, Beijing 100049, China

[6]Center for Environmental Systems Research, University of Kassel, Kassel, Germany

[7]Graduate School of Science and Technology, Hirosaki University, Hirosaki, Japan

[8]Institute of Physical Geography, Goethe-University Frankfurt, Altenhöferallee 1, 60438 Frankfurt, Germany

[9]Senckenberg Biodiversity and Climate Research Centre (SBiK-F), Senckenberganlage 25, 60325 Frankfurt, Germany

[10]Earth System Analysis, Potsdam Institute for Climate Impact Research (PIK), Potsdam, Germany

[11]Department of Civil and Environmental Engineering, Michigan State University, East Lansing, MI 48824 United States of America

[12]International Institute for Applied Systems Analysis, Laxenburg, Austria

[13]National Institute for Environmental Study, Tsukuba, Japan

Correspondence to: Qiuhong Tang (tangqh@igsnrr.ac.cn)

Table S1. Main characteristics of human impacts in the GHMs used in this study.

Model	**Water use**	**Dam and Reservoirs**	**Source of irrigation water withdrawal**
DBH	modeled irrigation	Use GRanD dataset, the number of dams and reservoirs varies according to the construction year for the VARSOC runs.	river, reservoirs
H08	modeled irrigation prescribed domestic and industrial water use	Use GRanD dataset, the number of dams and reservoirs varies according to the construction year for the VARSOC runs.	river, reservoirs, groundwater
LPJmL	modeled irrigation prescribed domestic, industrial and livestock	Use GRanD dataset, the number of dams and reservoirs varies according to the construction year for the VARSOC runs. Evaporation from reservoir surface is calculated.	river, reservoirs
MATSIRO	modeled irrigation prescribed domestic and industrial water use	Use GRanD dataset, the number of dams and reservoirs varies according to the construction year for the VARSOC runs.	river, reservoirs, groundwater
PCR-GLOBWB	modeled irrigation, domestic, industrial and livestock water use	Use GRanD dataset, the number of dams and reservoirs varies according to the construction year for the VARSOC runs. Evaporation from reservoir surface is calculated.	river, reservoirs, groundwater
WaterGAP2	modeled irrigation, domestic, industrial and livestock water use	Use GRanD dataset, the number of dams and reservoirs varies according to the construction year for the VARSOC runs. Evaporation from reservoir surface is calculated.	river, reservoirs, lakes, groundwater

Table S2. The Nash-Sutcliffe coefficients (NSE) for the simulated monthly streamflow from VARSOC experiment and observed monthly streamflow ($m^3 s^{-1}$) at the 44 stations over the 1971-2000 period. The observed mean annual streamflow (MAF, $m^3 s^{-1}$) averaged over the period is also shown for each station.

Number	**Station Name**	**MAF**	**NSE**	**River name**	**Number**	**Station Name**	**MAF**	**NSE**	**River name**
1	Guchengzi	151.26	-0.27	Songhua River	23	Xixian	117.87	0.31	Huai River
2	Fuyu	449.68	0.53	Songhua River	24	Fuyang	117.74	0.63	Huai River
3	Tonghe	1444.43	0.81	Songhua River	25	Lutaizi	639.00	0.80	Huai River
4	Kuerbin	26.94	0.004	Songhua River	26	Bengbu	800.63	0.81	Huai River
5	Chaoyang	18.00	-0.88	Liao River	27	Shishang	1968.28	0.93	Yangtze River
6	Chifeng	7.76	-0.25	Liao River	28	Changyang	431.02	0.75	Yangtze River
7	Tieling	84.36	<-1.0	Liao River	29	Pingshan	4546.38	0.77	Yangtze River
8	Liaozhong	101.43	0.50	Liao River	30	Sinan	910.98	0.79	Yangtze River
9	Changmapu	29.30	-0.37	Northwest Rivers	31	Cuntan	10747.92	0.68	Yangtze River
10	Yingluoxia	51.06	-0.26	Northwest Rivers	32	Datong	28460.19	0.78	Yangtze River
11	Zhamashenke	22.70	0.09	Northwest Rivers	33	Quzhou	207.66	0.80	Southeast Rivers
12	Sandaohezi	16.45	<-1.0	Hai River	34	Zhuji	40.24	0.58	Southeast Rivers
13	Panjiakou	60.87	0.01	Hai River	35	Zhuqi	1721.14	0.91	Southeast Rivers
14	Luanxian	96.09	0.71	Hai River	36	Yangkou	442.85	0.72	Southeast Rivers
15	Xiapu	4.58	<-1.0	Hai River	37	Daojieba	1746.97	0.12	Southwest Rivers
16	Huangbizhuang	32.14	-0.07	Hai River	38	Gulaohe	96.63	0.22	Southwest Rivers
17	Cetian	4.78	-0.01	Hai River	39	Manhao	310.84	0.82	Southwest Rivers
18	Lanzhou	976.80	0.53	Yellow River	40	Jiangbianjie	194.96	0.68	Pearl River
19	Shizuishan	867.25	0.45	Yellow River	41	Duanzhan	2005.11	0.88	Pearl River
20	Longmen	803.67	-0.47	Yellow River	42	Xiayan	449.63	0.82	Pearl River
21	Huayuankou	1103.51	0.09	Yellow River	43	Wuxuan	4130.25	0.81	Pearl River
22	Xianyang	107.26	0.63	Yellow River	44	Boluo	782.04	0.80	Pearl River

Table ~~S2~~S3. The proportions of river segments of China categorized by MAF changes. “<-10” in the header means the river segment showing MAF changes in [-20%, -10%), and so on.

	<-30	**<-20**	**<-10**	**<-5**	**<0**	**<5**	**<10**	**<20**	**<30**	**>=30**
ΔQ_c	2.56	5.24	16.32	13.47	16.42	15.76	10.55	6.84	3.55	9.29
ΔQ_h	2.28	1.00	3.83	9.04	54.27	26.80	1.29	0.85	0.13	0.50
ΔQ_a	3.13	7.13	17.11	13.40	16.29	15.69	9.86	5.87	3.83	7.69

Table ~~S3~~S4. Ensemble members of streamflow changes (ΔQ_a, % of MAF) between 1971-1990 and 1991-2010.

Forcing	**Model**	**CN**	**SH**	**LR**	**NW**	**HA**	**YR**	**HU**	**YZ**	**SE**	**SW**	**PR**
PGMFD v.2	H08	-1.21	-6.64	-0.85	19.89	-4.34	-2.29	1.71	-1.56	-4.67	2.35	1.96
	DBH	1.30	-4.29	-6.88	6.98	-13.29	-5.81	2.92	2.13	-1.48	5.77	3.10
	LPJmL	0.54	-3.06	-1.51	5.69	-9.79	-8.85	0.28	0.78	-3.22	2.68	3.81
	PCR-GLOBWB	-1.04	-7.51	-5.99	6.00	-7.80	-2.32	-5.50	-0.95	-2.95	3.13	0.79
	WaterGAP2	0.39	-3.16	-2.48	4.21	-11.09	-3.76	1.84	0.34	-4.30	3.85	1.81
	MATSIRO	-2.43	-10.04	-3.90	31.15	-6.60	-6.37	-0.51	-2.67	-4.94	1.77	-1.44
GSWP3	H08	-0.42	-5.26	-8.20	6.79	-14.20	-12.15	9.84	0.22	5.10	-0.23	3.57
	DBH	-0.66	-4.80	-12.31	16.98	-23.13	-10.53	3.09	0.47	0.99	2.30	-0.17
	LPJmL	-0.87	-2.67	-8.30	12.96	-13.56	-16.26	4.17	-0.21	2.52	-0.19	2.59
	PCR-GLOBWB	-2.14	-6.90	-8.17	11.08	-12.07	-7.35	-0.84	-1.43	1.37	0.60	-1.12
	WaterGAP2	-1.00	-3.34	-9.60	15.45	-21.38	-18.03	4.49	-0.46	1.49	0.28	0.31
	MATSIRO	1.09	0.73	-11.25	22.81	-33.18	-24.49	6.21	1.72	2.79	-1.13	2.37
WFDEI	H08	-6.74	-7.50	-6.16	4.51	-18.85	-14.18	3.31	-6.50	-4.76	-4.34	-6.75
	DBH	-6.38	-8.75	-11.96	-3.84	-26.26	-18.47	-4.47	-5.05	-3.46	-2.85	-6.48
	LPJmL	-4.12	-4.16	-7.66	8.27	-14.78	-16.88	0.61	-3.29	-4.59	-3.73	-4.84
	PCR-GLOBWB	2.82	-1.94	-1.93	31.61	-7.33	-0.83	-0.05	3.35	1.28	4.87	2.65
	WaterGAP2	-4.69	-4.77	-8.08	9.55	-22.00	-23.05	0.62	-3.88	-5.04	-3.87	-5.27
	MATSIRO	10.43	43.02	9.82	178.78	-0.42	27.95	11.69	11.24	2.80	5.33	4.04
All ensembles	Median	-0.93	-4.53	-7.27	10.32	-13.43	-9.69	1.78	-0.34	-2.22	1.19	1.30
	25^{th}	-2.36	-6.83	-8.28	6.20	-20.75	-16.72	0.03	-2.40	-4.52	-0.90	-1.36
	75^{th}	0.51	-3.09	-2.84	19.16	-8.30	-4.27	3.95	0.70	1.46	3.01	2.64

Table ~~S4~~S5. Ensemble members of streamflow changes induced by climate ~~change~~ variability (ΔQ_c, % of MAF) between 1971-1990 and 1991-2010.

Forcing	**Model**	**CN**	**SH**	**LR**	**NW**	**HA**	**YR**	**HU**	**YZ**	**SE**	**SW**	**PR**
PGMFD v.2	H08	-0.82	-6.55	-2.25	7.20	-7.06	-0.54	2.47	-0.99	-5.03	0.35	2.30
	DBH	2.31	-2.15	-2.55	11.29	-0.32	0.93	7.26	2.47	-0.96	3.76	3.05
	LPJmL	1.70	-1.99	0.33	4.41	-3.76	0.20	4.88	1.94	-2.87	0.12	4.43
	PCR-GLOBWB	0.33	-5.87	-3.44	1.09	-2.98	0.21	2.90	0.42	-2.24	1.34	2.23
	WaterGAP2	1.19	-2.73	-0.06	5.34	-3.93	-0.23	7.57	1.12	-3.86	2.04	2.47
	MATSIRO	-3.79	-13.87	-8.12	-5.06	-14.63	-20.25	-8.49	-3.69	-4.73	-2.05	-1.90
GSWP3	H08	0.02	-4.41	-8.83	10.51	-15.67	-10.08	11.16	0.72	4.85	-1.53	3.92
	DBH	0.63	-1.54	-1.94	28.33	-7.97	-5.12	8.66	0.93	1.42	2.02	-0.11
	LPJmL	0.39	-1.19	-4.20	16.21	-8.16	-8.63	9.36	0.75	2.83	-1.54	3.11
	PCR-GLOBWB	-0.72	-5.45	-5.20	10.00	-8.34	-5.57	6.40	-0.16	1.93	-0.05	0.21
	WaterGAP2	-0.08	-2.55	-6.78	27.65	-14.24	-15.34	11.99	0.39	1.94	-0.54	0.86
	MATSIRO	-0.77	-3.21	-16.35	12.44	-53.34	-40.28	5.67	0.19	3.03	-3.49	1.70
WFDEI	H08	-6.12	-7.13	-6.60	5.11	-19.75	-11.21	4.52	-5.75	-5.03	-5.93	-6.47
	DBH	-4.87	-6.37	-6.11	2.70	-13.98	-12.34	1.91	-4.00	-2.90	-4.28	-6.02
	LPJmL	-2.73	-2.91	-4.42	12.00	-10.50	-9.73	6.45	-1.97	-4.10	-4.83	-4.04
	PCR-GLOBWB	4.71	-0.30	1.13	30.71	-2.89	1.44	7.22	4.99	1.97	4.93	4.05
	WaterGAP2	-3.77	-4.03	-5.46	17.37	-15.51	-18.55	8.14	-2.93	-4.44	-5.38	-4.47
	MATSIRO	-1.28	1.25	-6.82	96.98	-13.82	-20.52	4.85	-0.40	-0.52	-3.67	-3.94
All ensembles	Median	-0.29	-3.06	-4.81	17.86	-9.42	-9.35	6.43	0.17	-1.60	0.55	1.28
	25th	-2.24	-5.77	-6.73	11.71	-14.53	-14.85	4.61	-1.89	-4.04	-1.17	-3.43
	75th	0.49	-2.03	-2.32	33.21	-4.71	-0.51	7.99	0.76	1.94	2.82	2.90

Table ~~S5~~S6. Ensemble members of streamflow changes induced by DHI change (ΔQ_h, % of MAF) between 1971-1990 and 1991-2010.

Forcing	**Model**	**CN**	**SH**	**LR**	**NW**	**HA**	**YR**	**HU**	**YZ**	**SE**	**SW**	**PR**
PGMFD v.2	H08	-0.42	-0.09	1.39	-2.93	2.72	-1.51	-0.76	-0.44	0.36	-0.06	-0.34
	DBH	-0.98	-2.13	-4.33	-6.68	-12.98	-6.49	-4.35	-0.20	-0.52	-0.08	0.06
	LPJmL	-1.40	-1.07	-1.85	-2.53	-6.03	-8.76	-4.60	-1.11	-0.35	-0.27	-0.62
	PCR-GLOBWB	-1.32	-1.64	-2.55	-0.93	-4.83	-2.24	-8.39	-1.12	-0.71	-0.19	-1.44
	WaterGAP2	-0.86	-0.43	-2.42	-4.40	-7.15	-3.28	-5.73	-0.67	-0.44	-0.05	-0.66
	MATSIRO	1.09	3.83	4.22	-4.91	8.03	14.39	7.98	1.10	-0.21	0.01	0.45
GSWP3	H08	-0.51	-0.85	0.63	-5.07	1.47	-1.88	-1.33	-0.44	0.25	-0.05	-0.35
	DBH	-1.12	-3.26	-10.37	-12.44	-15.16	-5.24	-5.57	-0.31	-0.43	-0.08	-0.06
	LPJmL	-1.31	-1.48	-4.10	-4.66	-5.40	-7.31	-5.19	-0.87	-0.31	-0.25	-0.52
	PCR-GLOBWB	-1.14	-1.45	-2.97	-1.63	-3.72	-1.59	-7.24	-0.95	-0.56	-0.15	-1.33
	WaterGAP2	-0.93	-0.79	-2.82	-12.67	-7.13	-2.33	-7.50	-0.79	-0.45	-0.03	-0.54
	MATSIRO	1.59	3.94	5.10	-6.67	20.16	16.41	0.54	1.57	-0.25	0.17	0.67
WFDEI	H08	-0.65	-0.37	0.44	-4.36	0.89	-2.76	-1.21	-0.58	0.26	-0.05	-0.28
	DBH	-1.45	-2.38	-5.85	-5.73	-12.28	-5.93	-6.38	-0.87	-0.56	-0.05	-0.46
	LPJmL	-1.43	-1.25	-3.24	-6.81	-4.28	-6.81	-5.84	-1.13	-0.49	-0.30	-0.80
	PCR-GLOBWB	-1.32	-1.63	-3.06	-3.35	-4.44	-1.98	-7.27	-1.07	-0.69	-0.16	-1.40
	WaterGAP2	-1.03	-0.73	-2.62	-12.11	-6.48	-4.21	-7.52	-0.86	-0.60	-0.02	-0.79
	MATSIRO	11.57	41.77	16.64	-5.89	13.41	49.06	6.84	11.98	3.32	7.34	7.98
All ensembles	Median	-1.04	-0.96	-2.58	-7.96	-4.63	-2.60	-5.38	-0.74	-0.44	-0.07	-0.49
	25^{th}	-1.40	-1.60	-3.20	-15.58	-6.97	-5.84	-7.03	-0.96	-0.55	-0.19	-0.76
	75^{th}	-0.57	-0.39	0.58	-5.90	1.33	-1.71	-1.24	-0.35	-0.22	-0.05	-0.11

Table ~~S6~~S7. Ensemble medians, 25th and 75th percentiles of MAF changes (%) induced by DHI change (ΔQ_h) from 1971-1980 to 1981-1990, 1991-2000, and 2001-2010, respectively. All ΔQ_h values are percentages of the MAF from VARSOC simulations over the 1971-1980 period.

Period / Region	**1981-1990**			**1991-2000**			**2001-2010**		
	ΔQ_h	ΔQ_h_25th	ΔQ_h_75th	ΔQ_h	ΔQ_h_25th	ΔQ_h_75th	ΔQ_h	ΔQ_h_25th	ΔQ_h_75th
CN	-0.37	-0.58	0.05	-0.65	-1.39	0.89	-1.62	-1.94	-0.78
SHJ	-1.78	-2.02	-0.34	-1.46	-2.01	-0.97	-2.15	-2.57	-1.47
LR	-3.43	-4.38	-0.23	-2.30	-3.18	1.92	-5.21	-8.29	-3.67
NW	-6.09	-8.15	-4.18	-8.99	-13.12	-4.58	-13.53	-25.40	-9.97
HA	-2.81	-7.40	-0.98	-4.49	-6.58	2.09	-7.07	-10.65	1.89
YR	-7.49	-13.76	-3.83	-4.10	-6.46	-1.83	-8.95	-10.95	-3.71
HU	-1.97	-3.74	-0.03	-5.53	-7.41	-2.20	-7.01	-10.35	-0.54
YZ	0.05	-0.19	0.64	-0.38	-0.93	1.39	-0.73	-1.18	0.37
SE	-0.32	-0.42	-0.16	-0.37	-0.58	-0.18	-0.85	-1.01	-0.46
SW	-0.03	-0.06	-0.01	-0.07	-0.19	-0.04	-0.08	-0.30	-0.06
PR	-0.31	-0.54	-0.14	-0.75	-1.32	-0.22	-0.42	-0.78	-0.19

Table S7S8. Relative contributions of DHI from previous studies. ΔQ_a denotes the relative contribution of DHI and is computed as $100\times\Delta Q_h/\Delta Q_a$ in the studies. Period 1 denotes the period without (or with little) human impact, Period 2 denotes the period with human impact. Period 2 is blank when no sub-periods were used in the study.

Major River	**River**	**ΔQ_a (%)**	**Period 1**	**Period 2**	**Station**	**Latitude**	**Longitude**	**Catchment area (km^2)**	**Reference**
Hai River	Qinlong River	-41.5	1957-1979	1980-2000	Taolinkou	40.13	119.05	5060	Bao et al., 2012
	Bai River	-59.9	1954-1979	1980-2004	Zhangjiafen	40.62	116.78	8506	
	Zhang River	-73.9	1951-1972	1973-2004	Guantai	36.33	114.08	17800	
	Chao River	-68.6	1961-1966, 1973-1979	1980-2001		41.00	117.00	6716	Wang et al., 2009
	Bai River	-70.4	1961-1966, 1973-1979	1980-2001		40.55	116.50	9072	
Yellow River	Upper reaches	-37	1956-1989	1990-2000	Tangnaihai	35.50	100.15	121972	Zhao et al., 2009
	Upper reaches	-46	1968-1986	1987-2000	Lanzhou	36.07	103.82	222551	
	Upper reaches	-44	1960-1970	1991-2000	Baimasi	34.72	112.58	13915	Wang et al., 2010
	Wuding River	-84.3	1961-1971	1972-1997	Baijiachuan	37.24	110.42	30261	Li et al., 2007
	Wuding River	-23	1961-2005		Baijiachuan	37.24	110.42	30261	Yuan et al. 2018
Huai River	Upper reaches	-45	1960-2010		Bengbu	32.95	117.27	270000	Ma et al., 2014

Reference

Bao, Z., Zhang, J., Wang, G., Fu, G., He, R., Yan, X., Jin, J., Liu, Y., and Zhang, A.: Attribution for decreasing streamflow of the Haihe River basin, northern China: Climate variability or human activities?, J. Hydrol., 460-461, 117-129, 10.1016/j.jhydrol.2012.06.054, 2012.

Li, L., Zhang, L., Wang, H., Wang, J., Yang, J., Jiang, D., Li, J., and Qin, D.: Assessing the impact of climate variability and human activities on streamflow from the Wuding River basin in China, Hydrol. Processes, 21, 3485-3491, doi:10.1002/hyp.6485, 2007.

~~Ma, F., Ye, A., Gong, W., Mao, Y., Miao, C., and Di, Z.: An estimate of human and natural contributions to flood changes of the Huai River, Global Planet. Change, 119, 39-50, 10.1016/j.gloplacha.2014.05.003, 2014.~~

~~Wang, G., Xia, J., and Chen, J.: Quantification of effects of climate variations and human activities on runoff by a monthly water balance model: A case study of the Chaobai River basin in northern China, Water Resour. Res., 45, doi:10.1029/2007WR006768, 2009.~~

~~Wang, J., Hong, Y., Gourley, J., Adhikari, P., Li, L., and Su, F.: Quantitative assessment of climate change and human impacts on long-term hydrologic response: a case study in a sub-basin of the Yellow River, China, Int. J. Climatol., 30, 2130-2137, doi:10.1002/joc.2023, 2010.~~

~~Yuan, X., Jiao, Y., Yang, D., and Lei, H.: Reconciling the Attribution of Changes in Streamflow Extremes From a Hydroclimate Perspective, Water Resour. Res., doi:10.1029/2018WR022714, 2018.~~

~~Zhao, F., Xu, Z., Zhang, L., and Zuo, D.: Streamflow response to climate variability and human activities in the upper catchment of the Yellow River Basin, Sci. China Ser. E: Technol. Sci., 52, 3249, 10.1007/s11431-009-0354-3, 2009.~~

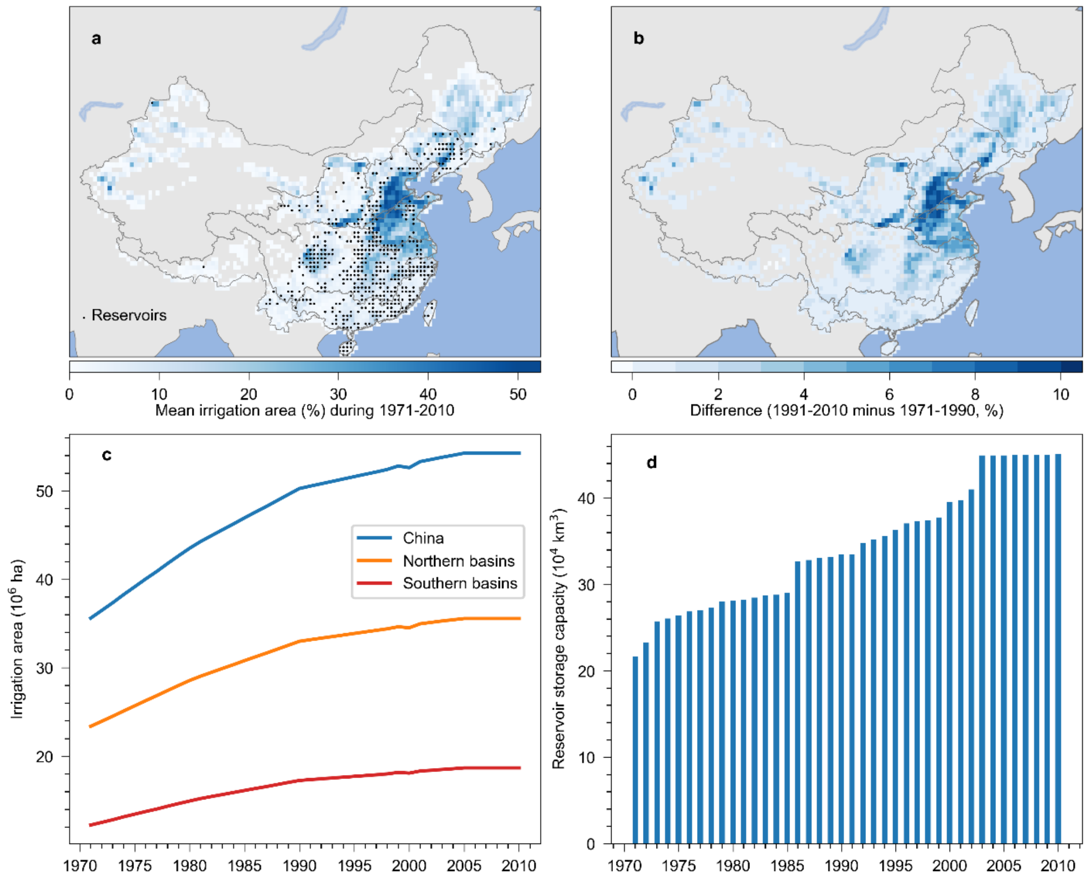

Figure S1. Irrigated areas (Fader et al., 2010; Portmann et al., 2010) and reservoirs (Lehner et al., 2011) in China used in the ISIMIP2a VARSOC experiment. (a): mean irrigation area per grid cell (%) over the 1971-2010 period and locations of reservoir; (b): difference in mean irrigation area between the periods of 1971-1990 and 1991 and 2010; (c): annual irrigation area for China, northern basins, and southern basins; (d): annual storage capacity of reservoirs in China. The areas without irrigation are not shown on the map.

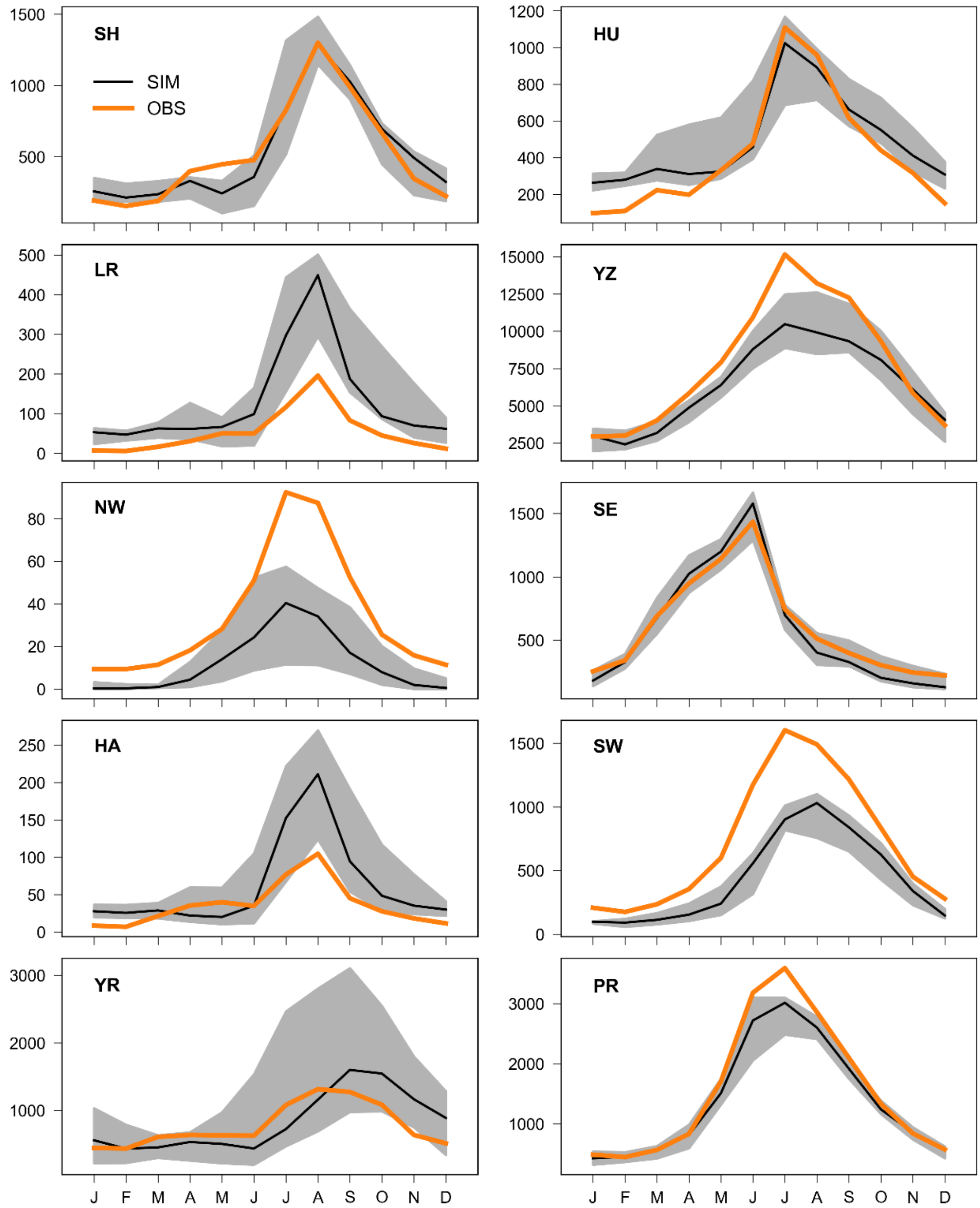
SH
SIM
OBS
HU
LR
YZ
NW
SE
HA
SW
YR
PR
J F M A M J J A S O N D
J F M A M J J A S O N D

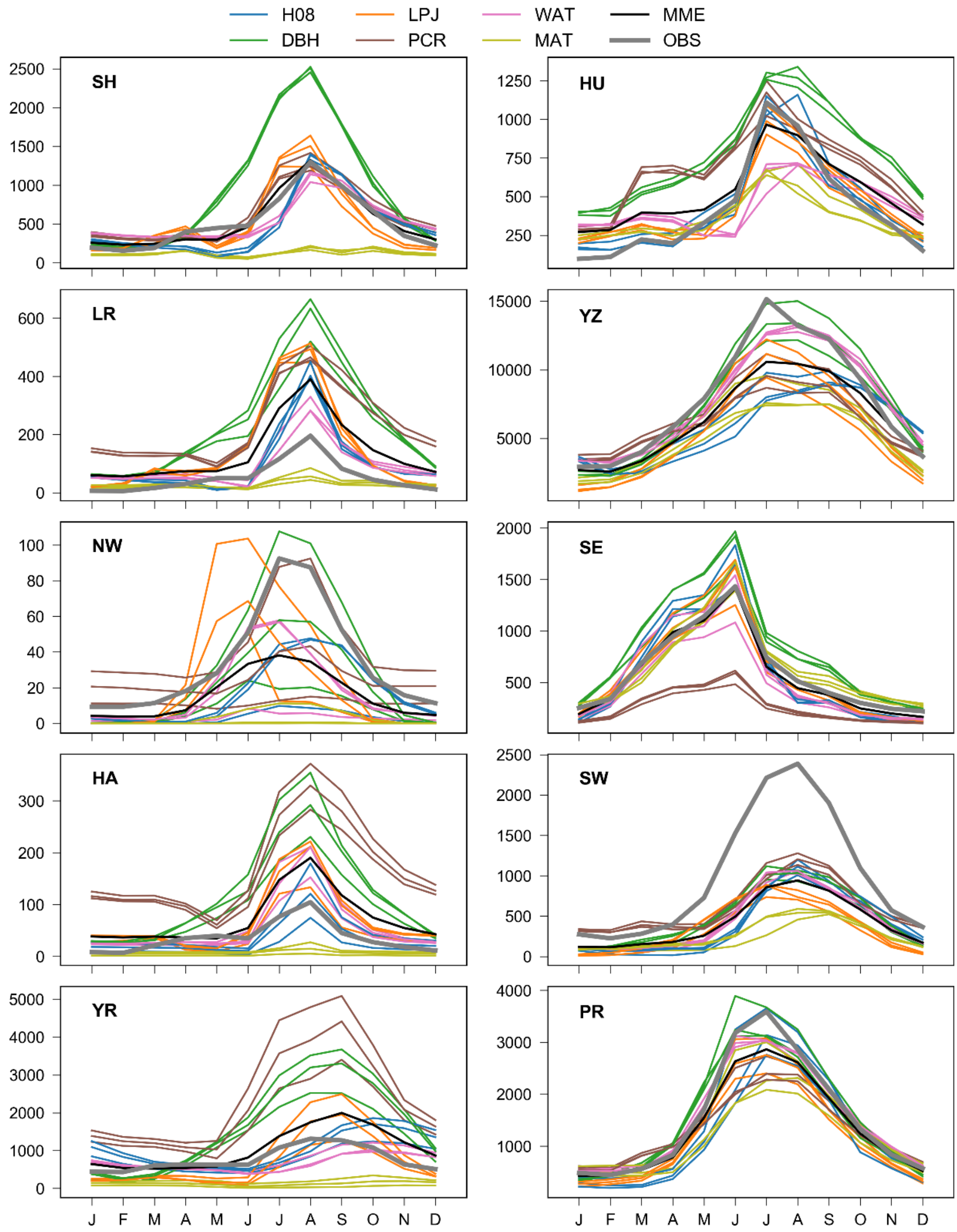

Figure S2. The seasonal cycle of streamflow from observations and GHMs. The seasonal observations are based on monthly streamflow and averaged for the hydrological stations in each basin (Figure 1). The simulations are averaged values over the grid cells identified by the location of stations. H08: H08 model; DBH: DBH model; LPJ: LPJmL model; PCR: PCR-GLOBWB model; WAT: WaterGAP model; MAT: MATSIRO model; MMS: multimodel medians; SIM indicates simulations and OBS: indicates observations. The grey areas show the 25th and 75th percentiles of the multimodel simulations. Northern basins: Songhua River (SH), Liao River (LR), Northwest Rivers (NW), Hai River (HA), Yellow River (YR), Huai River (HU); Southern basins: Yangtze River (YZ), Southeast Rivers (SE), Southwest Rivers (SW), Pearl River (PR).

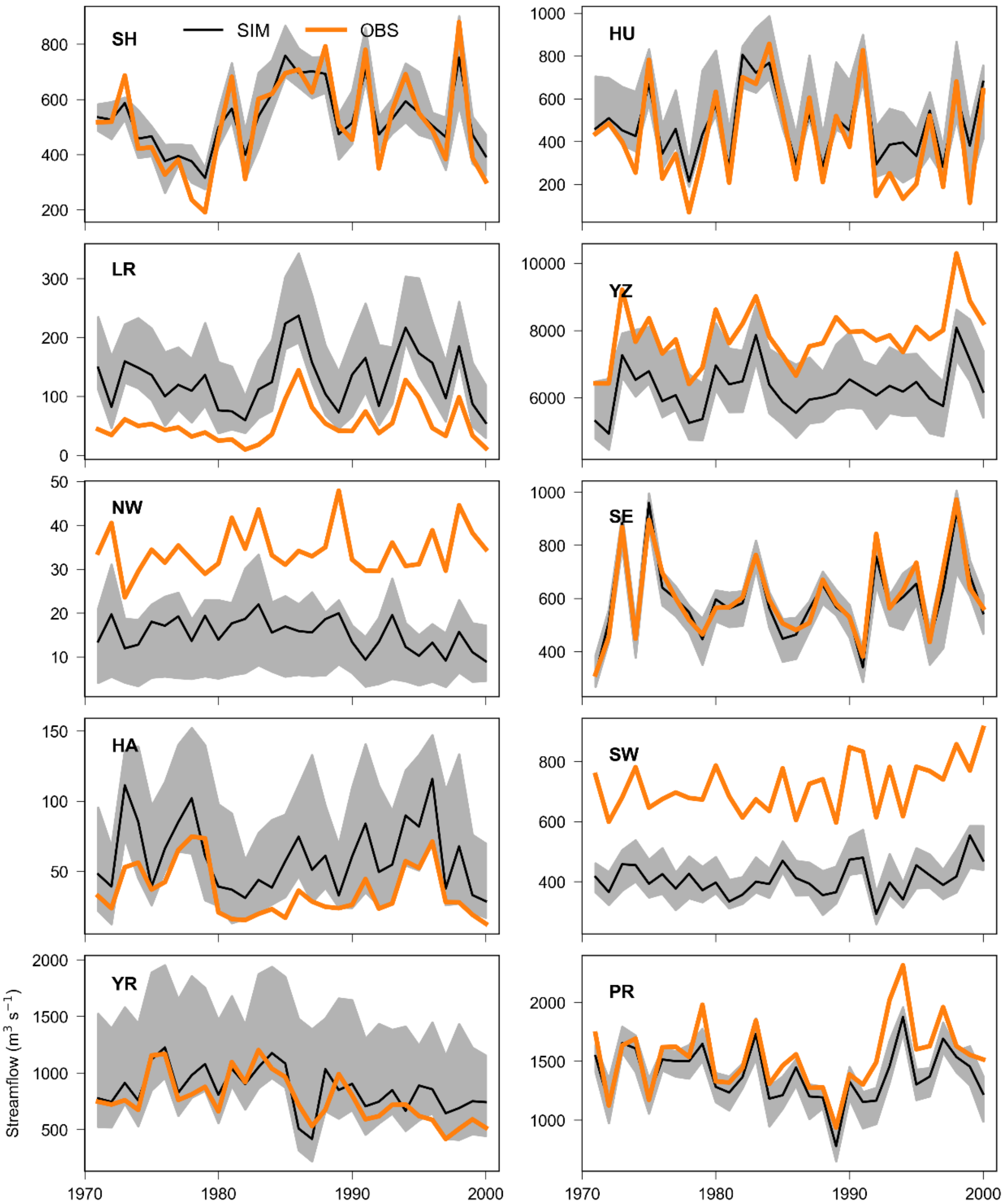

Figure S3. Simulated (black) and observed (orange) mean annual streamflow at the hydrological stations in each basin. The observations are the average values of the hydrological stations, while the simulations are averaged values over the grid cells identified by the location of stations. The grey areas show the 25th and 75th percentiles of the multimodel simulations.

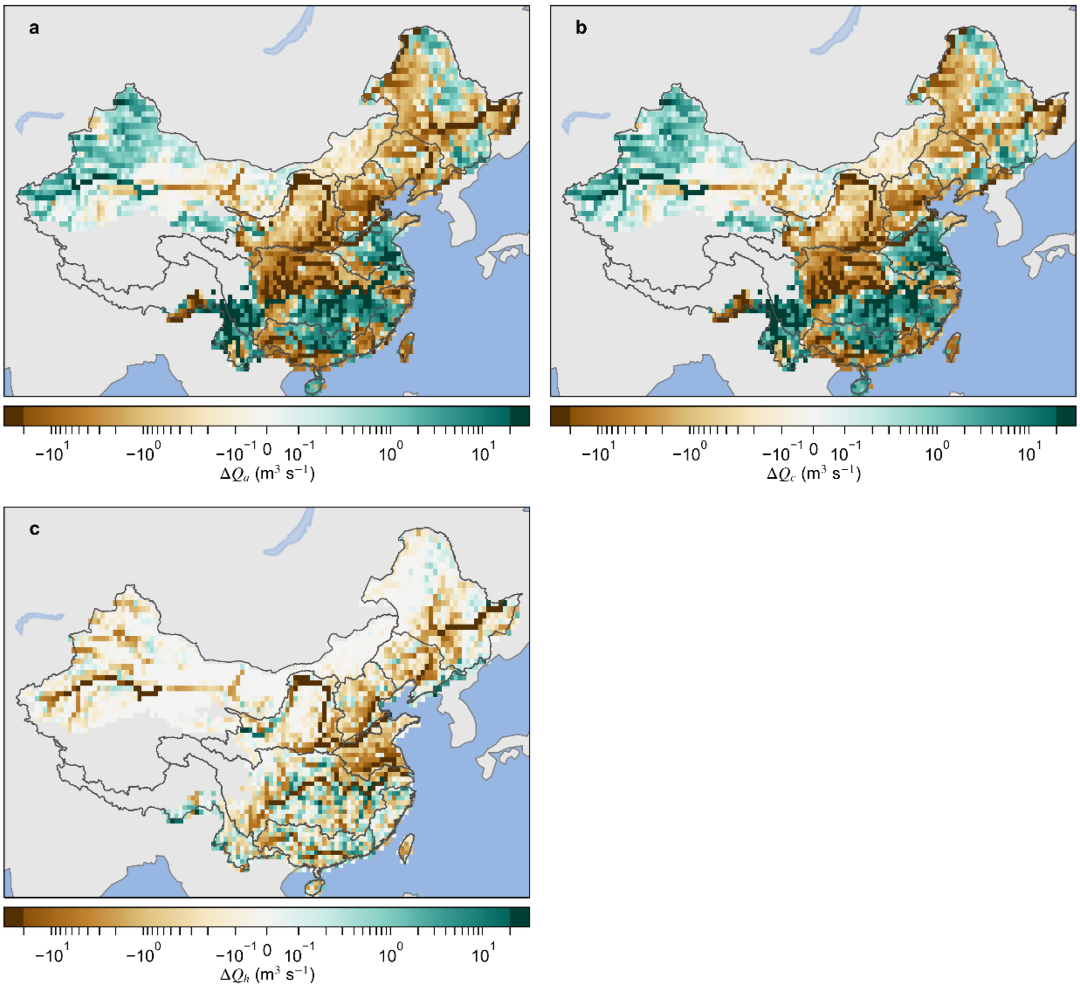

Figure ~~S3~~S4. MAF changes (m^3 s^{-1}) over China between the sub-periods 1971-1990 and 1991-2010. (a) Total MAF changes (ΔQ_a), (b) MAF changes induced by climate ~~change~~ variability (ΔQ_c) and (c) MAF changes induced by DHI change (ΔQ_h).

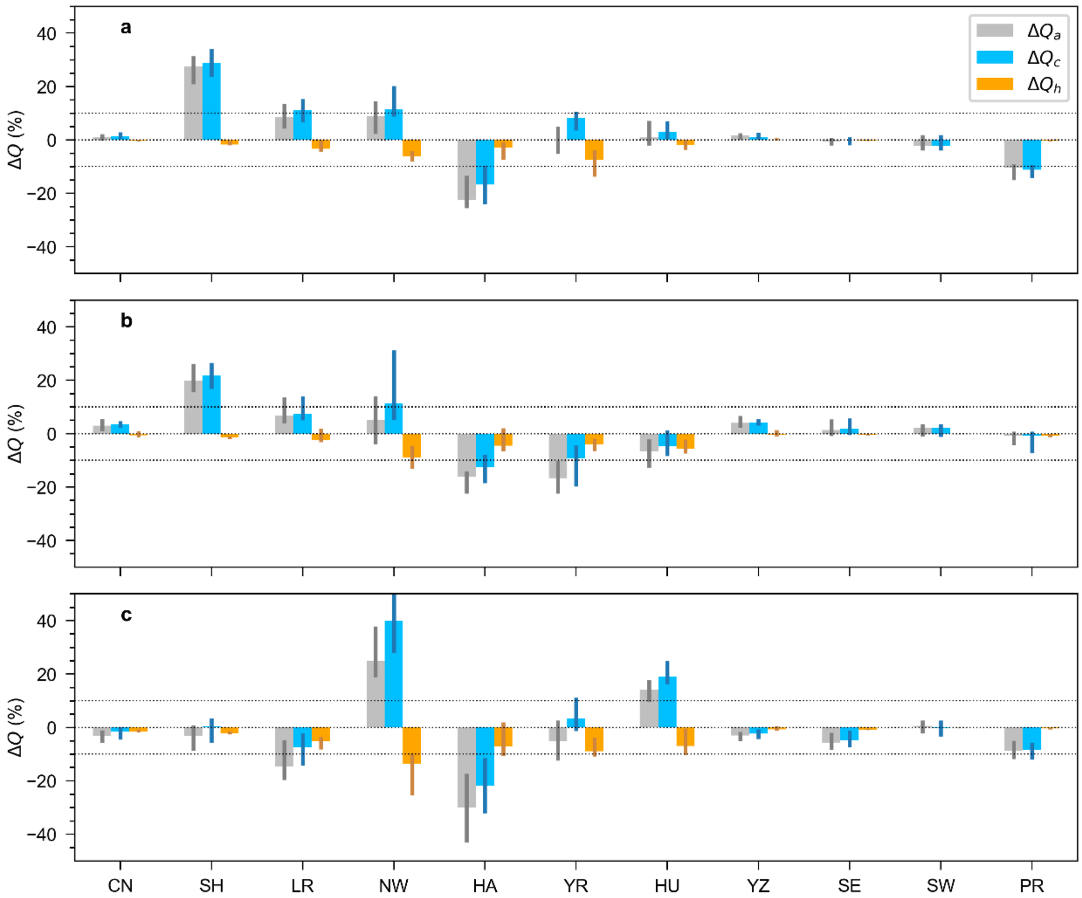

Figure ~~S4~~S5. Total MAF change (ΔQ_a), MAF change induced by climate ~~change~~ variability (ΔQ_c), and MAF change induced by DHI change (ΔQ_h) from the period 1971-1980 to (a) 1981-1990, (b) 1991-2000 and (c) 2001-2010, respectively. The bars show the medians and the error bars show the range of 25th and 75th of MAF changes.

Reference

Bao, Z., Zhang, J., Wang, G., Fu, G., He, R., Yan, X., Jin, J., Liu, Y., and Zhang, A.: Attribution for decreasing streamflow of the Haihe River basin, northern China: Climate variability or human activities?, J. Hydrol., 460-461, 117-129, 10.1016/j.jhydrol.2012.06.054, 2012.

Fader, M., Rost, S., Müller, C., Bondeau, A., and Gerten, D.: Virtual water content of temperate cereals and maize: Present and potential future patterns, J. Hydrol., 384, 218-231, 10.1016/j.jhydrol.2009.12.011, 2010.

Lehner, B., Liermann, C. R., Revenga, C., Vörösmarty, C., Fekete, B., Crouzet, P., Döll, P., Endejan, M., Frenken, K., Magome, J., Nilsson, C., Robertson, J. C., Rödel, R., Sindorf, N., and Wisser, D.: High-resolution mapping of the world's reservoirs and dams for sustainable river-flow management, Frontiers in Ecology and the Environment, 9, 494-502, 10.1890/100125, 2011.

Li, L., Zhang, L., Wang, H., Wang, J., Yang, J., Jiang, D., Li, J., and Qin, D.: Assessing the impact of climate variability and human activities on streamflow from the Wuding River basin in China, Hydrol. Processes, 21, 3485-3491, doi:10.1002/hyp.6485, 2007.

Ma, F., Ye, A., Gong, W., Mao, Y., Miao, C., and Di, Z.: An estimate of human and natural contributions to flood changes of the Huai River, Global Planet. Change, 119, 39-50, 10.1016/j.gloplacha.2014.05.003, 2014.

Portmann, F. T., Siebert, S., and Döll, P.: MIRCA2000—Global monthly irrigated and rainfed crop areas around the year 2000: A new high-resolution data set for agricultural and hydrological modeling, Global Biogeochem. Cycles, 24, GB1011, 10.1029/2008GB003435, 2010.

Wang, G., Xia, J., and Chen, J.: Quantification of effects of climate variations and human activities on runoff by a monthly water balance model: A case study of the Chaobai River basin in northern China, Water Resour. Res., 45, doi:10.1029/2007WR006768, 2009.

Wang, J., Hong, Y., Gourley, J., Adhikari, P., Li, L., and Su, F.: Quantitative assessment of climate change and human impacts on long-term hydrologic response: a case study in a sub-basin of the Yellow River, China, Int. J. Climatol., 30, 2130-2137, doi:10.1002/joc.2023, 2010.

Yuan, X., Jiao, Y., Yang, D., and Lei, H.: Reconciling the Attribution of Changes in Streamflow Extremes From a Hydroclimate Perspective, Water Resour. Res., doi:10.1029/2018WR022714, 2018.

Zhao, F., Xu, Z., Zhang, L., and Zuo, D.: Streamflow response to climate variability and human activities in the upper catchment of the Yellow River Basin, Sci. China Ser. E: Technol. Sci., 52, 3249, 10.1007/s11431-009-0354-3, 2009.